IOP Publishing Environ. Res. Lett. 17 (2022) 093006 https://doi.org/10.1088/1748-9326/ac8944

ENVIRONMENTAL RESEARCH
LETTERS

OPEN ACCESS

RECEIVED
29 March 2022

REVISED
11 August 2022

ACCEPTED FOR PUBLICATION
12 August 2022

PUBLISHED
9 September 2022

TOPICAL REVIEW

Theoretical and paleoclimatic evidence for abrupt transitions in the Earth system

Niklas Boers[1,2,3,*], **Michael Ghil**[4,5] **and Thomas F Stocker**[6,7]

[1] Earth System Modelling, School of Engineering & Design, Technical University of Munich, Munchen, Germany
[2] Potsdam Institute for Climate Impact Research, Telegraphenberg A31, 14473 Potsdam, Germany
[3] Department of Mathematics and Global Systems Institute, University of Exeter, Exeter, United Kingdom
[4] Geosciences Department and Laboratoire de Météorologie Dynamique (CNRS and IPSL), Ecole Normale Supérieure and PSL University, Paris, France
[5] Department of Atmospheric and Oceanic Science, University of California at Los Angeles, Los Angeles, CA, United States of America
[6] Climate and Environmental Physics, Physics Institute, University of Bern, 3012 Bern, Switzerland
[7] Oeschger Center for Climate Change Research, University of Bern, 3012 Bern, Switzerland
[*] Author to whom any correspondence should be addressed.

E-mail: boers@pik-potsdam.de

Keywords: abrupt transitions, tipping points, nonlinear climate dynamics, Earth system, bifurcations

Abstract

Specific components of the Earth system may abruptly change their state in response to gradual changes in forcing. This possibility has attracted great scientific interest in recent years, and has been recognized as one of the greatest threats associated with anthropogenic climate change. Examples of such components, called tipping elements, include the Atlantic Meridional Overturning Circulation, the polar ice sheets, the Amazon rainforest, as well as the tropical monsoon systems. The mathematical language to describe abrupt climatic transitions is mainly based on the theory of nonlinear dynamical systems and, in particular, on their bifurcations. Applications of this theory to nonautonomous and stochastically forced systems are a very active field of climate research. The empirical evidence that abrupt transitions have indeed occurred in the past stems exclusively from paleoclimate proxy records. In this review, we explain the basic theory needed to describe critical transitions, summarize the proxy evidence for past abrupt climate transitions in different parts of the Earth system, and examine some candidates for future abrupt transitions in response to ongoing anthropogenic forcing. Predicting such transitions remains difficult and is subject to large uncertainties. Substantial improvements in our understanding of the nonlinear mechanisms underlying abrupt transitions of Earth system components are needed. We argue that such an improved understanding requires combining insights from (a) paleoclimatic records; (b) simulations using a hierarchy of models, from conceptual to comprehensive ones; and (c) time series analysis of recent observation-based data that encode the dynamics of the present-day Earth system components that are potentially prone to tipping.

1. Introduction: tipping points, bifurcations, and all that

It has been known for six decades that nonlinearities in the dynamics of the Earth's climate system and of its components can in principle lead to abrupt transitions (Stommel 1961, Veronis 1963, Lorenz 1963a). Such jumps in behavior can occur in response to external forcing, even if the latter varies only gradually, and it may also be the result of self-sustained, oscillatory dynamics (Ghil and Childress 1987, Ghil and Lucarini 2020, Riechers *et al* 2021).

For abrupt state transitions to occur, a system must possess more than one stable steady state. First hints that this might be the case for the Earth's climate came from studies of the Earth's radiation budget in the 1970s. These studies revealed that a nonlinear temperature dependence of the albedo—with a colder planet having more ice and thus a higher albedo—can lead to two stable states for given values of incoming

solar radiation. The second stable state is considerably colder than the stable state associated with the present climate and it was called, at first, a 'deep freeze' and, later, a *snowball Earth* (Held and Suarez 1974, Ghil 1976, North *et al* 1979, Ghil and Lucarini 2020).

For some time after its theoretical discovery, this cold state had been considered as a mere theoretical figment of too simple a climate model. It was found, however, also in a general circulation model (GCM) (Wetherald and Manabe 1975); and, quite some time later, it became clear that in the Earth's deep past, some 650 million years ago, such a snowball Earth state had indeed occurred, possibly more than once (Hoffman *et al* 1998, 2017, Hoffmann *et al* 2010). Over the course of the last decades, several abrupt climate transitions have been identified in paleoclimate proxy records, from glacial terminations (Crucifix 2018, Bagniewski *et al* 2021, Riechers *et al* 2021) to millennial-scale abrupt shifts during previous glacial intervals (Johnsen *et al* 1992, Dansgaard *et al* 1993) and abrupt climate events during the Holocene (Bond *et al* 2001), such as the desertification of the Sahara and North Atlantic ice rafting events that had profound impacts on the tropical monsoon system and early human civilizations (Gibbons 1993, Stanley *et al* 2003). Some instances of past abrupt climate transitions of the last 30 kyr and their impacts on different Earth system components have recently been reviewed in Brovkin *et al* (2021).

The mounting paleoclimate evidence suggests that similar abrupt transitions might also occur in the future, possibly in response to the anthropogenic release of greenhouse gases and the resulting atmospheric warming. To assess the risk of future abrupt climate transitions, the main tools available are numerical models that simulate Earth's climate system dynamics in greater or lesser detail. A hierarchy of such models (Ghil 2001, Held 2005) can be crudely classified into the following categories: (a) simple energy-balance models (EBMs) that simulate temperature variations in response to the Earth's energy budget, i.e. the difference between ingoing and outgoing radiation (Budyko 1969, Sellers 1969); (b) conceptual models of isolated processes and box models resolving interactions between different regions of the atmosphere and oceans (Stommel 1961); (c) so-called Earth System Models of Intermediate Complexity (EMICs), which have mostly been used for paleoclimate simulations in recent years (Stocker *et al* 1992, Claussen *et al* 2002); (d) GCMs that integrate the partial differential equations governing the dynamics of the atmosphere and oceans on a discretized spatial grid of increasing resolution (Ghil 2001); and, finally, (e) comprehensive Earth System Models (ESMs) that simulate the coupled dynamics of atmosphere, oceans, ice sheets and sea ice, the carbon cycle, and land-surface and vegetation dynamics. The latter is the class of models used for the most recent sixth assessment report (AR6) of the Intergovernmental Panel on Climate Change (IPCC) (IPCC 2021a).

In the summary for policymakers of the IPCC's AR6 (IPCC 2021b), it is stated that *Abrupt responses and tipping points of the climate system, such as strongly increased Antarctic ice-sheet melt and forest dieback, cannot be ruled out (high confidence)*. The careful phrasing of these statements is, on the one hand, due to the conservative and consensus-seeking way in which the IPCC's ARs are written: recall that the 'I' in 'IPCC' stands for the political, multi-government oversight of its activities and reports. On the other hand, such statements are careful because the uncertainties are huge.

It is not yet clear whether available climate and ESMs capture the highly nonlinear dynamics that would lead to abrupt transitions with an accuracy that suffices to provide reliable estimates of the critical forcing levels. For instance, models closer to the high end of the hierarchy have had problems in reproducing abrupt climate shifts documented in paleoclimate proxy records (Valdes 2011). Only very recently has there been some progress in simulating abrupt climate transitions from the past with the class of comprehensive models that are used for the IPCC's future projections (Peltier and Vettoretti 2014, Klockmann *et al* 2020, Hopcroft and Valdes 2021).

Transferring the insights gained from paleoclimate studies to future climate conditions with higher greenhouse gas concentrations is challenging, and there remain huge disagreements in the projected responses of nonlinear Earth system components, such as the Atlantic Meridional Overturning Circulation (AMOC) (Stouffer *et al* 2006, Weijer *et al* 2019, Jackson and Wood 2020, Boers 2021) or the Amazon rainforest (Boysen *et al* 2020, Parsons 2020, Almazroui *et al* 2021). In particular, there are still large uncertainties in the estimates of the critical forcing levels at which tipping of different nonlinear Earth system components might occur.

Actually, even the disagreement among different IPCC-class models for the equilibrium climate sensitivity (ECS)—i.e. the equilibrium response of globally averaged temperature to a doubling of atmospheric greenhouse gas concentrations—remains large. Based on models alone, the likely ECS uncertainty still equals or exceeds the 1.5°–4.5° range (IPCC 2013) given by the Charney-led assessment in the late 1970s (Charney *et al* 1979), and it is not far from the estimate of Arrhenius at the end of the 19th century (Arrhenius 1896). Given such uncertainties in the extent of future warming, even if future greenhouse gas concentrations were known accurately—and given that estimating the critical forcing levels of the nonlinear Earth system is far from obvious—it is clear that we are far from reliable estimates of when abrupt climate transitions in response

to ongoing anthropogenic warming might be set in motion.

The purpose of this review paper is to make available to as large a scientific audience as possible the ingredients of a more solidly based assessment of when such drastic events might occur and with what uncertainties. We will focus mainly on climate transitions that are abrupt on time scales relevant for humans, thus excluding most potential deep-time paleoclimate transitions that took more than thousands of years to unfold.

The paper is organized as follows. We summarize in the next section basic concepts and methods of dynamical system theory that can help describe abrupt transitions, in a self-contained mathematical framework. In particular, tipping points, bifurcations, nonautonomous and random dynamical systems, and the concept of critical slowing down will be introduced. In section 3, we turn our attention to the empirical evidence of abrupt climate transitions in past climates, as obtained from different kinds of paleoclimate proxy archives. Our evidence focuses on the glacial–interglacial cycles of the Pleistocene, the Dansgaard–Oeschger (DO) events of previous glacial intervals, and the Bond events of the Holocene. In section 4, we describe briefly several components of the Earth system that have been proposed as likely candidates for abrupt state transitions in response to ongoing anthropogenic global warming. Some recent successes in modeling abrupt climate transitions are mentioned in section 4.5, and we conclude in section 5 with final remarks and an outlook.

2. Dynamical system theory for Earth system science

2.1. Dynamical systems and bistability

Assume that the state of a system of interest can be described by a vector $\mathbf{x} \in \mathbb{R}^d$ and that the time evolution of $\mathbf{x}(t)$ is governed by the following equation of motion, namely a first-order autonomous ordinary differential equation:

$$\dot{\mathbf{x}} = \mathbf{f}(\mathbf{x}; p). \tag{1}$$

Here $(\cdot)^{\cdot} = \mathrm{d}(\cdot)/\mathrm{d}t$, $\mathbf{f}$ denotes a generally nonlinear, smooth—i.e. continuously differentiable, up to some order—vector field and p a scalar parameter or, in more general cases, a small set of parameters. For clarity, one separates the variables $\mathbf{x}$ from the parameter p by a semi-colon. The term 'autonomous' refers to the fact that in equation (1) both the coefficients and the forcing are constant in time. This means that changes in p are assumed to be infinitely slow or, at least, very slow compared to the characteristic internal-variability times of the system being modeled.

Points $\mathbf{x}^*$ for which $\mathbf{f}(\mathbf{x}^*; p) = 0$ are called fixed points. Linearizing the equation of motion around a given fixed point $\mathbf{x}^*$ yields, for a small perturbation $\tilde{\mathbf{x}} = \mathbf{x} - \mathbf{x}^*$,

$$\dot{\tilde{\mathbf{x}}} = \mathbf{f}'(\mathbf{x}^*; p)\tilde{\mathbf{x}}; \tag{2}$$

here $\mathbf{f}'(\mathbf{x}^*; p)$ is the Jacobian matrix comprised of the elements $\partial f_i/\partial x_j$. For an initial condition $\tilde{\mathbf{x}}_0$, the solution to this linearized equation is given by

$$\tilde{\mathbf{x}}(t) = \mathrm{e}^{\mathbf{f}'t}\tilde{\mathbf{x}}_0\,. \tag{3}$$

We call a fixed point $\mathbf{x}^*$ linearly stable if all eigenvalues of $\mathbf{f}'$ have negative real part, and linearly unstable otherwise. A scalar example will be given in the next subsection.

The bifurcations of a dynamical system that we deal with in this subsection describe the creation and annihilation of fixed points, as well as changes in their linear stability. Further types of bifurcations are considered in the next subsection.

Typically, bifurcations lead to abrupt qualitative changes in the dynamics, explaining why they are often invoked as a mathematical model for abrupt regime shifts or state transitions in real-world systems. Until recently, bifurcations were studied mostly in the context of autonomous dynamical systems. The more realistic situations in which the forcing is allowed to depend explicitly on time are addressed in section 2.3. In this broader context, the abrupt transitions that are caused by bifurcations have been identified as one of several types of *tipping* (Ashwin *et al* 2012).

In fact, there is some confusion between two interpretations of the term tipping: (a) a mathematically accepted one, following Ashwin *et al* (2012), and (b) one in which the term ?tipping point? designates a level of forcing at or near which an abrupt transition occurs. The latter interpretation follows Gladwell (2000) and Lenton *et al* (2008). We return to both of them in section 2.3.

2.1.1. The double-well potential as a source of bistability

As an instructive and widely used example, we briefly introduce a prototype model to describe scalar dynamical systems than can occupy either one of two stable fixed points, separated by an unstable one, as plotted in figure 1(a). The double-well potential $U(x; p) = x^4/4 - x^2/2 - px$ leads to the equation of motion

$$\dot{x} = U'(x; p) = -x^3 + x + p, \tag{4}$$

where $U' = \partial U/\partial x$. For $p < -p^*$ this dynamical system has only the stable fixed point x^*_- and for $p > p^*$ it has only the stable fixed point x^*_+, while for $-p^* < p < p^*$ the two stable fixed points $x^*_\pm$ coexist and there is a third, unstable fixed point in-between these two, x^*_0.

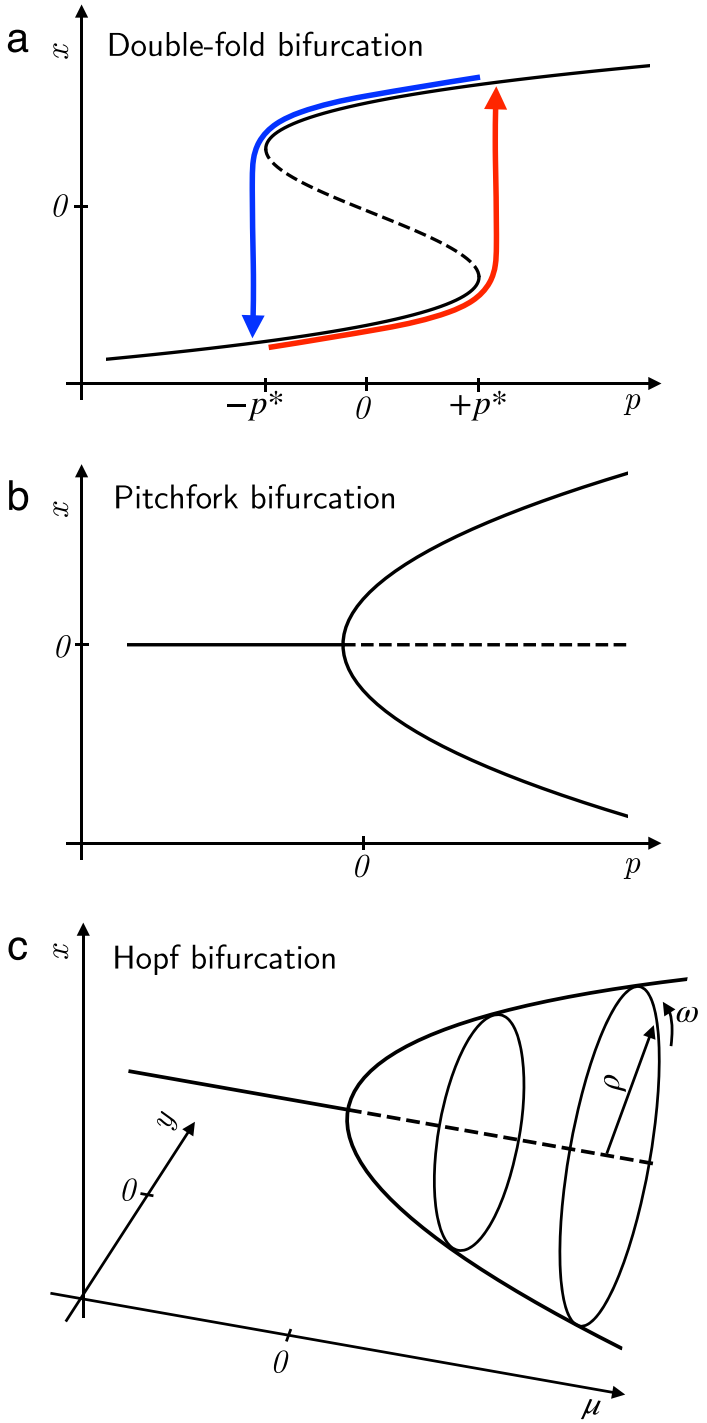

Figure 1. Bifurcation diagrams for (a) the double-fold; (b) supercritical pitchfork; and (c) supercritical Hopf bifurcation. Stable fixed-point branches are indicated by solid lines, unstable ones by dashed lines. The colored lines in panel (a) correspond to a hysteresis cycle. See text for details.

The two stable fixed points correspond to the two minima of the potential U above, whereas $\pm p^*$ are the two critical thresholds of the system. In this scalar case, the basins of attraction of the two minima are the intervals $-\infty < x < x_0^*$ and $x_0^* < x < +\infty$, respectively. They are separated by the unstable fixed point x_0^*, which is a local maximum of the potential $U(x)$.

Changing p slowly from, say, $p = -1$ to $p = +1$ will lead to a bifurcation-induced critical transition from x_-^* to x_+^* at the critical value $p = p^*$. When p is subsequently changed back from $p = 1$ to $p = -1$, the transition from x_+^* back to x_-^* will only occur at $p = -p^*$. This phenomenon of jumps from one fixed point to the other occurring at distinct parameter values is called *hysteresis*, and it is highly relevant to the practical reversibility of abrupt transitions. It was first studied in mechanical systems by J C Maxwell and it is important in the study of various types of magnetism. In the context of climate science, a hysteresis loop like the one seen in figure 1(a) has been described in

detail for EBMs (Ghil and Childress 1987, Ghil 1994), using solar insolation as the parameter p.

The bifurcation introduced above is called a *double-fold bifurcation*, since it is obtained by combining a *supercritical* fold, with the stable branch reaching forward, to $p \to \infty$, with a *subcritical* one, with the stable branch reaching backward, to $p \to -\infty$. A more recent version of such a double-fold bifurcation is plotted in figure 2 of Von der Heydt *et al* (2016) for an EBM with respect to carbon dioxide concentration as the parameter p.

2.1.2. Bistability in the presence of symmetry: the pitchfork bifurcation

Another example of bistability is given by a pitchfork bifurcation (figure 1(b)). Its so-called *normal form*, i.e. the simplest ordinary differential equation that exhibits the change of behavior of interest, is

$$\dot{x} = x(p - x^2). \tag{5}$$

This bifurcation captures bistable behavior in systems in which spatial mirror symmetry prevails for low p-values. A well-known example in the climate sciences is symmetry in a meridional plane for an idealized AMOC at low buoyancy forcing by a weak pole-to-equator temperature and precipitation gradient (Quon and Ghil 1992, Ghil 2001, Dijkstra 2005). In this case, water sinks at both poles and rises on either side of the equator, forming two overturning cells that are symmetric with respect to the equatorial plane.

The solutions of equation (5) are $x_0 = 0, x_\pm = \pm\sqrt{p}$. In this normal form, the scalar symmetry of the latter two solutions with respect to 0 stands for the mirror symmetry of the AMOC's overturning cells with respect to the equator.

The bifurcation occurs as the parameter p, which is a normalized form of the forcing in the AMOC case, crosses over from negative to positive values. It is easy to check that, for $p \leqslant 0$, $x_0 = 0$ is the unique fixed point, while for $p > 0$ the three fixed points coexist. Their linear stability is given by considering infinitesimal perturbations around a given steady-state solution $x = x_* + \xi$.

With the scalar version $f = f(x;p)$ of the notation in equation (1), we have the scalar version of equation (2) in the specific case at hand given by

$$(x_* + \xi)^{\cdot} = f(x_* + \xi; p) = 0 + \left.\frac{\partial f(x;p)}{\partial x}\right|_{x=x_*} \times \xi + \mathcal{O}(\xi^2) \simeq p - 3x_*^2.$$

Since $\dot{x}_* = 0$, this leaves

$$\dot{\xi} = p - 3x_*^2 \tag{6}$$

to determine linear stability for small ξ (Ghil and Childress 1987, Dijkstra and Ghil 2005). Thus it is clear that, for $p < 0$, the unique solution $x_* = 0$ is linearly stable; but, for $p > 0$, this null solution becomes linearly unstable, while the two mutually symmetric solutions $x_* = x_\pm = \pm\sqrt{p}$ are stable, since $p - 3p < 0$. We thus suspect that, for sufficiently strong buoyancy forcing the two-cell AMOC will lose its stability and yield the approximately single-cell AMOC that is currently observed; see Stocker and Wright (1991), Quon and Ghil (1992)and section 4.2 below.

2.2. Beyond bistability: limit cycles, tori and chaos

Bistability is only the first step up the bifurcation tree that leads from system behavior with the highest degree of symmetry in space and time—possibly as simple as uniform in both—to behavior that has greater and greater complexity (Eckmann 1981, Ghil and Childress 1987, Strogatz 2018). We outline now one further step up this tree, the one leading from fixed points to stable periodic solutions, called limit cycles in dynamical system parlance.

2.2.1. Hopf bifurcation and the transition to oscillatory solutions

This step can be understood by considering the normal form of a *Hopf bifurcation* in the (x, y)-plane, as illustrated in figure 1(c).

In polar coordinates, this normal form is given by

$$\dot{\rho} = \rho(\mu - \rho^2), \quad \dot{\theta} = \omega, \tag{7}$$

with $\omega = -1$ for uniform anticlockwise rotation around the origin. The two equations above are decoupled and the one for the radial variable $\rho = x^2 + y^2$ has exactly the same form as the pitchfork normal form for x in equation (5). Note, though, that here ρ is necessarily nonnegative and the mirror symmetry of figure 1(b) is replaced by the rotational symmetry of figure 1(c).

2.2.2. Successive bifurcations and routes to chaos

A further step on the route to chaos for deterministic systems with no explicit time dependence (Eckmann 1981, Ghil and Childress 1987, Strogatz 2018) involves the transition from a one-dimensional (1D) limit cycle to a two-dimensional torus in phase space. In the latter case, the motion on the torus is quasi-periodic—i.e. the coordinates of the point on the torus are of the form $x(t) = f(\omega_1 t, \omega_2 t), y(t) = g(\omega_1 t, \omega_2 t)$, where the functions $f(s,t), g(s,t)$ are arbitrary and the two angular frequencies ω_1 and ω_2 are incommensurable, i.e. ω_1/ω_2 is not a rational number. This kind of motion is typical in celestial mechanics (Ghil and Childress 1987, Arnold *et al* 2007) and, in fact, the periodicities that are associated with the orbital forcing of the glacial-interglacial cycles in section 3.3 are of this type, although one usually refers to them by truncated values—such as those in table 12.1 of Ghil and Childress (1987)—that could suggest that the ratios between these periodicities, like

41 kyr for the obliquity and 19 kyr for the precessional parameter, do have a common denominator.

Quasi-periodic motion looks much more irregular than purely periodic motion. Thus, for instance, the intervals between lunar or solar eclipses are highly irregular. Still, the 14th century scholar Nicole Oresme was already aware of the kinematic consequences of quasi-periodicity for celestial motions (Grant 1961). He realized that a periodic and a quasi-periodic motion cannot be distinguished from each other during a finite observation interval. Oresme also knew that the motion of a point on a torus will describe a simple closed loop if the two angular velocities are commensurable, while the point's orbit will never close, but densely cover the surface of the torus if the two velocities are incommensurable (Arnold 2012), i.e. in a way that is visually indistinguishable from painting the whole torus a uniform color.

From quasi-periodic motion to a deterministically chaotic one, there are several routes (Eckmann 1981), some of which were explored numerically in the climate sciences by Lorenz (1963a, 1963b)and described more didactically in chapters V and VI of Ghil and Childress (1987) for atmospheric motions, and in the paleoclimatic context in its chapter XII, as well as in Ghil (1994). We shall not go into greater detail herein, but pass instead to the more recent insights from the theory of dynamical systems subject to time-dependent forcing.

2.3. Non-autonomous and random dynamical systems

Realistically, the natural systems that we want to describe in terms of dynamical system theory are non-autonomous, meaning that $\mathbf{f}$ in equation (1) above has an explicit time dependence. The Earth system as a whole, as well as all its components, is clearly non-autonomous, being affected by time-dependent forcing such as quasi-periodic variations in solar insolation due to gravitational perturbations in Earth's orbit (Milankovitch 1920), along with anthropogenic forcing due to rising greenhouse gas concentrations (Arrhenius 1896, IPCC 2013, 2021a).

Moreover, there is typically high-frequency forcing—such as cloud processes or weather variability—that is, in a drastic simplification, often represented by white noise (Hasselmann 1976). Including both deterministic and stochastic time dependence requires a description of the dynamics in terms of stochastic differential equations of the form

$$\mathrm{d}\mathbf{X} = \mathbf{F}(\mathbf{X}, t; p)\mathrm{d}t + \sigma(\mathbf{X})\mathrm{d}\mathbf{W}\,, \qquad (8)$$

where $\mathrm{d}\mathbf{W}$ denotes the infinitesimal increments of a Wiener process, which are stationary and independently distributed according to a normal distribution with mean $\mu = 0$ and variance $\mathbb{E}(\mathrm{d}\mathbf{W}^2) = \mathrm{d}t$. Often, a further simplification is made in assuming that the noise is additive or state-independent, and thus $\sigma =$ const. above.

The possibly time-dependent, but still deterministic term $\mathbf{F}(\mathbf{X}, t; p)$ is called the drift. The theory of random dynamical systems—including specifically a nonlinear interaction between the deterministic drift and random processes, as in equation (8) above—has been applied to the climate sciences only recently (Ghil *et al* 2008, Chekroun *et al* 2011, Bódai and Tél 2012).

Ashwin *et al* (2012) have proposed three classes of abrupt transitions in systems that can be described by equation (8): (a) bifurcation-induced transitions, (b) noise-induces transitions, and (c) rate-induced transitions. An example of the first class has already been given in section 2.1 and figure 1(a) above.

For an example of the second class, assume that the control parameter p remains constant in the drift term of equation (8), which is taken again to correspond to a double-well potential, as in equation (4). Noise-induced transitions occur when the noise amplitude is sufficiently high for the system to switch occasionally, and unpredictably, from one potential well to the other. Moreover, when p varies so as to push the system toward a bifurcation point, the noise will cause it to transition before—and, in certain cases, long before—the critical parameter value p^* of the corresponding deterministic system is reached.

Finally, the third class of rate-induced transitions arises when there is no strong separation between the system's intrinsic time scales and those at which the control parameter changes. So far, we implicitly assumed that, for each change in p, the system has sufficient time to adapt to the new equilibrium position; this type of slow change in p is sometimes called quasi-adiabatic. If this is not the case, the fixed point attracting the system may change its position so quickly that the system cannot follow and eventually loses track of the basin of attraction in which it started and falls into the other one (Ashwin *et al* 2012).

Ashwin *et al* (2012) refer to the three types of tipping described above as B-tipping, N-tipping and R-tipping. Thus, aside from the rhetorically striking character of tipping points, the latter classification can be seen as the mathematically well-defined generalization of the bifurcations that have been treated in autonomous dynamical systems for a long time, to the non-autonomous and random setting. Thus, B-tipping is not totally novel inasmuch as it only adds deeper insight to what happens when a parameter p changes at a finite, rather than infinitely slow rate. N-tipping, in turn, is a well-known phenomenon that has been widely studied in physics, chemistry and biology (Horsthemke and Lefever 1984), as well as in the climate sciences (Sura 2002). The biggest surprises

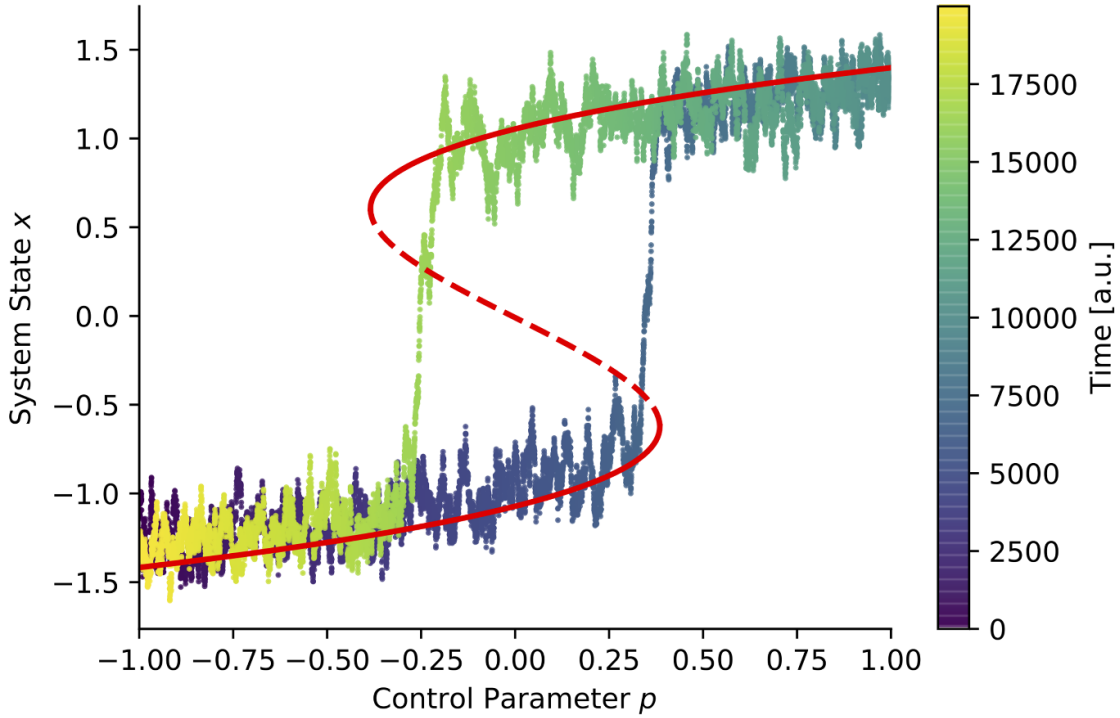

Figure 2. Sketch of a double-fold bifurcation and how it leads to abrupt transitions and hysteresis in the temporal evolution of a system in a double-well potential with slowly changing parameter, driven by additive white noise. The stable branch of fixed points is indicated by solid red, the unstable one by dashed red. For example, simple EBMs (Ghil and Lucarini 2020) exhibit a bifurcation structure of this kind, with the system state in that case given by global mean temperatures and the control parameter given by the solar constant. The upper stable branch corresponds then to the current climate state, while the lower one corresponds to the so-called Snowball Earth state (Held and Suarez 1974, Ghil 1976, Ghil and Lucarini 2020).

occur for R-tipping (Wieczorek *et al* 2011, Feudel *et al* 2018, Ghil 2019, Pierini and Ghil 2021).

There are even more complex types of critical transitions that involve two different kinds of behavior that are not separated by a basin boundary at all. Such an example was described in detail by Chekroun *et al* (2018) for a delay differential model of the well-known El Niño–Southern oscillation phenomenon. In this model, the time-dependent pullback attractor that characterizes non-autonomous and random dynamical systems undergoes a crisis that consists of a chaos-to-chaos transition. This crisis manifests itself by a brutal change in the size and shape of the pullback attractor, but not in its position in phase space.

We illustrate in figure 2 a simple combination of B-tipping and N-tipping of a system governed by $\mathrm{d}x = U'(x;p)\mathrm{d}t + \sigma \mathrm{d}W$, with U as in equation (4) and $\mathrm{d}W$ as in equation (8), but $\sigma =$ const. In this case, the parameter p changes slowly, as suggested already in figure 1(a), but the noise causes the transition to occur before p reaches the critical value. For example, simple EBMs (Ghil and Lucarini 2020) exhibit a double-fold bifurcation of this kind, as described already in section 2.1 above. The upper stable branch corresponds in this case to the current climate state, while the lower one corresponds to the Snowball Earth state (Held and Suarez 1974, Ghil 1976, Ghil and Lucarini 2020).

To obtain the system trajectory simulated in detail in figure 2, the control parameter p is varied slowly from $+1$ to -1 and back to $+1$, causing the system to transition first from the upper stable branch to the lower one, and then, at considerably higher p, back to the upper stable branch. Note that due to the noise driving the system, transitions do occur typically earlier than expected from the corresponding deterministic dynamics governed by equation (4).

2.4. Critical slowing down

As noted in the section 1, it remains unclear how reliable even the most comprehensive climate and ESMs are in representing the dynamics governing highly nonlinear components of the Earth system. Given that this uncertainty translates into a lack of predictability of the critical forcing levels at which an abrupt transition may be expected, it is necessary to devise other ways to estimate the stability of a given subsystem, and how this stability might change in the course of time due to a change in the forcing. If sufficiently long observational data encoding the dynamics are available, one possibility is to exploit the data. Fortunately, a system's gradual loss of stability can be traced in the statistical properties of a time series generated by the system, for several classes of bifurcations (Carpenter and Brock 2006, Dakos *et al* 2008, Scheffer *et al* 2009, Bury *et al* 2020).

Taking the simplest, scalar case of equation (8) and linearizing its drift around a stable fixed point X^* gives rise to a linear Ornstein–Uhlenbeck process with damping rate λ,

$$\mathrm{d}\tilde{X} = \lambda \tilde{X}\mathrm{d}t + \sigma \mathrm{d}W, \tag{9}$$

where we used the tilde notation of equation (2) for the small deviation from X^*. Note that the dynamics is stable only if $\lambda < 0$, with stability lost as λ crosses zero from below.

Discretizing a realization of this Ornstein–Uhlenbeck process into finite time steps Δt yields an autoregressive process. The variance $\langle \tilde{X}^2 \rangle$ and the autocorrelation $\alpha(n)$ at lag n of this process are given by

$$\langle \tilde{X}^2 \rangle = -\frac{\sigma^2}{1 - \mathrm{e}^{2\lambda\Delta t}}, \quad \alpha(n) = \mathrm{e}^{n\lambda\Delta t}. \tag{10}$$

Hence, as the system approaches the critical threshold where λ reaches zero, the variance will diverge and the lag-one autocorrelation will increase toward one; this is commonly referred to as *critical slowing down*.

The increases in λ—as well as in the variance and in the autocorrelations at different lags, based on the above expressions—can be used to anticipate the approaching of a B-tipping, as defined in section 2.3 above. The above derivation remains valid for all local bifurcations of codimension 1 (Bury *et al* 2020), i.e. those that only involve a scalar parameter p, as discussed in connection with figure 1 in sections 2.1 and 2.2. The expressions for variance and autocorrelation remain those of equation (10) in the case of both pitchfork and transcritical bifurcations, in which one still only deals with changes in the number or stability of steady states (Strogatz 2018).

In the case of a supercritical Hopf bifurcation, like the one of figure 1(c), one has a transition from a steady state to a stable periodic solution and the real scalar λ is replaced by the real part of a complex conjugate pair of eigenvalues—see again section 2.2—but the expression for the variance in equation (10) remains unchanged. The autocorrelation, however, depends in this case on the underlying frequency ω of the oscillations as well, i.e. $\alpha(n) = \mathrm{e}^{n\lambda\Delta t}\cos\omega n\Delta t$. Hence, depending on the relationship between the lag time $n\Delta t$ and the period $T = 2\pi/\omega$ of the oscillations, $\alpha(n)$ can either increase or decrease. For $n\Delta t < T/4$, $\alpha(n)$ will increase on the way to the Hopf bifurcations; but for $n\Delta t \approx T/2$, it will decrease because effectively one computes the correlation between out-of-phase signals with increasing amplitudes toward the bifurcation point (Bury *et al* 2020).

The fluctuation–dissipation theory underlying this phenomenon of critical slowing down goes back to Kubo's seminal work (Kubo 1966) and it has been used in many other inspiring ways in the Earth sciences (Ghil 2019, Ghil and Lucarini 2020) and elsewhere. It is only quite recently, though, that the results of this theory for $\lambda \nearrow 0$ in equations (9) and (10) have started to be applied to obtain an empirical warning for forthcoming critical transitions in natural systems (Carpenter and Brock 2006, Dakos *et al* 2008, Scheffer *et al* 2009). Several authors have shown that abrupt climate transitions in the remote past were preceded by statistical changes that can be attributed to critical slowing down (Dakos *et al* 2008, Rypdal 2016, Boers 2018, Boettner *et al* 2021).

The assumption of a scalar system can be easily dropped by carrying out first a principal component analysis (Jolliffe 2002, Held and Kleinen 2004), and then focussing on the linear mode with the largest variance. The condition of additive white noise is less trivial. There have recently been some extensions of the theory to time-correlated noise (Boers 2021, Boettner and Boers 2022, Kuehn *et al* 2022). If the noise is state-dependent, though, knowledge of the actual dependence is needed to still be able to identify critical slowing down, for example by including the changes in the noise characteristics that are induced by the state dependence.

A concept that is closely associated with a system's stability is its resilience; it is commonly defined as the system's ability to recover from external perturbations. By globally comparing recovery rates—estimated empirically from remotely sensed vegetation data—to lag-one autocorrelation and variance estimates, it has been shown that the latter two estimates can indeed serve as metrics for vegetation resilience. Based on these metrics, an almost globally coherent loss of vegetation resilience during the last two decades has been inferred (Smith *et al* 2022).

Moreover, it has recently been suggested that several tipping elements of the climate system—i.e. subsystems of the latter that are particularly at risk of incurring an abrupt transition (Lenton *et al* 2008)—show first signs of a stability loss in observational time series for these elements. The data sets in question include ice core-based melt data from the central-western part of the Greenland ice sheet (Boers and Rypdal 2021), reanalysis-based sea-surface temperature (SST) and salinity fingerprints of the AMOC strength (Boers 2021), as well as the remotely sensed, high-resolution vegetation indices for the Amazon rainforest (Boulton *et al* 2022).

3. Empirical evidence for abrupt transitions in past climates

3.1. Snowball Earth

Even relatively simple, spatially 1D models of the Earth's energy balance predict two alternative stable states, as soon as a nonlinear temperature-dependent albedo is introduced—motivated by the simple fact that there's more ice at lower temperatures (Budyko 1969, Sellers 1969). As mentioned already in the section 1, the warmer one of these stable states represents current climate conditions, while the colder

one was termed a 'deep freeze' when theoretically predicted (Held and Suarez 1974, Ghil 1976, North *et al* 1979) and *Snowball Earth* when empirically confirmed (Ghil and Lucarini 2020); recall also figure 2 herein.

This bistability has only relatively recently been found and described in paleoclimate proxy records, which demonstrate convincingly that the snowball state was actually attained some 650 Myr ago (Hoffman *et al* 2002, 2017, Pierrehumbert 2005). Coupled atmosphere–ocean models have, moreover, uncovered recently an even richer structure of equilibrium states, depending on solar irradiation and obliquity, in the context of exoplanet climate studies (Kilic *et al* 2017, 2018).

3.2. Eocene–Oligocene transition

The Eocene–Oligocene transition involves the shift from an almost ice-free to a so-called icehouse planet (Summerhayes 2015) that occurred approximately 34 Myr ago. It can, for example, be inferred from a relatively sharp decline in benthic δ^{18}O, together with a sharp increase of benthic δ^{13}C in the recent CENOGRID composite record (Westerhold *et al* 2020). The key feature of this shift is Antarctica's first glaciation (Hutchinson *et al* 2021).

Unfortunately, given how far back in time this transition occurred, the data base is quite sparse, and unlikely to allow unique identification of the underlying mechanisms. Indeed, for some other deep-time paleoclimate events, the available proxy records proved sufficient to at least determine whether these events were preceded by critical slowing down or not (Boettner *et al* 2021). The time resolution and quality of the data around the Eocene–Oligocene transition, though, did not allow one to decide this issue (Boettner *et al* 2021). In particular, the respective roles of atmospheric carbon dioxide concentrations and astronomical forcing for this transition are accordingly still subject to debate (Ladant *et al* 2014, Kennedy *et al* 2015).

3.3. Glacial-interglacial cycles

Global transitions between glacial and interglacial climate states occurred roughly every 100 kyr during the last one million years. More than a century ago, orbitally induced insolation variations have been proposed as an explanation of the Earth system's glacial-interglacial cycles (Milankovitch 1920). These variations in solar insolation are caused, in turn, by changes in the Earth's orbit around the Sun and in the inclination of its axis of rotation. They involve periodicities of 19 kyr and 21 kyr in precession, of 41 kyr in obliquity, and several periodicities grouped around 100 kyr and 400 kyr in eccentricity (Berger 1978). But the periodicities around 100 kyr are far from dominant (Ghil and Childress 1987, Ghil 1994).

Widespread consensus exists that the orbital variations do act as a pacemaker of the glacial-interglacial cycles (Hays *et al* 1976, Imbrie and Imbrie 1986). Nevertheless, the exact interplay of the Earth system's intrinsic and highly nonlinear variability with the Milankovitch forcing is still a matter of debate (Ghil 1994, Huybers 2009, Riechers *et al* 2021). One substantial puzzle is the highly nonlinear, sawtooth-shaped character of the glacial-interglacial cycles during the Late Pleistocene, roughly since 800 kyr b2k, with very rapid 'terminations' (Broecker and van Donk 1970, Ghil and Childress 1987) and quite slow returns to colder conditions. These terminations involve rapid increases in global temperatures, as well as sudden drops in global ice volume; see figure 3(a) herein.

Among the theories advanced to explain the so-called '100 kyr problem' stochastic resonance is well known (Benzi *et al* 1981, 1982, Nicolis 1981). It relies on the joint effects of a purely periodic forcing, a coexistence of two stable steady states of the climate model, and just the right amount of noise. The two steady states have to be much closer than those associated with the present climate and a Snowball Earth, just a few degrees apart. But the response is perfectly symmetric, with equally abrupt jumps from the interglacial to the glacial state and back. Thus, this theory cannot explain the marked asymmetry between warming and cooling in the 100 kyr cycle.

Rather than appealing to bistability, in one form or another, it might be more plausible to think of various highly nonlinear oscillators of fast-slow type, like the van der Pol (van der Pol 1920, 1926) or FitzHugh–Nagumo (FitzHugh 1961, Nagumo *et al* 1962) oscillator. Such oscillators capture asymmetrically fast vs. slow changes in their variables and have been used widely to model electric circuits as well as neural impulses. Further details on these oscillators and how to use them in paleoclimatic modeling can be found in Riechers *et al* (2021) and in section 3.6 herein.

To the questions about (a) how the approximate 100 kyr periodicity arises, given a complicated power spectrum of the orbital forcing and (b) the asymmetry in the slow waxing and fast waning of ice sheets at this periodicity one has to add (c) how this periodicity becomes dominant during the last Myr, given that the forcing has dominant spectral peaks around roughly 41 kyr (obliquity) and 21 kyr (precession), but comparably weak peaks (due to eccentricity) in the vicinity of 100 kyr peak. It is the latter question that is discussed in the next subsection.

3.4. Mid-Pleistocene transition (MPT)

A prominent mode change in the global climate of the past two million years is the MPT. Between 1.2 Myr and 0.8 Myr ago, the pacing of the ice ages changed from a roughly 40 kyr, obliquity-dominated cyclicity to much slower, roughly 100 kyr cycles with a significantly larger amplitude. The latter near-periodicity seems to coincide roughly with the time scale of eccentricity variations of the Earth's orbit, but a direct

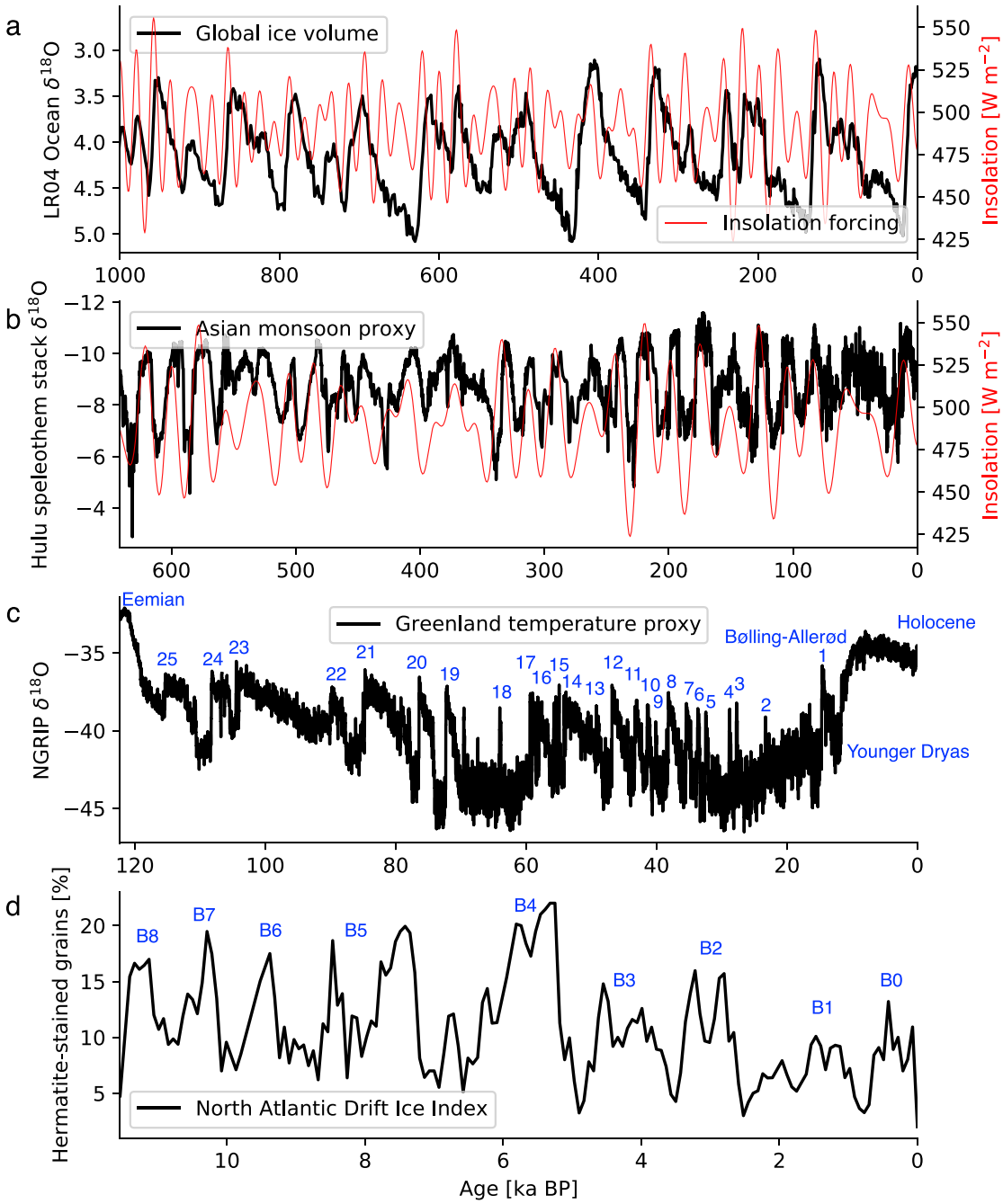

Figure 3. Time series from paleoclimate proxy reconstructions that show abrupt climate transitions. Summer insolation at 65° N (red) in panels (a) and (b); δ^{18}O (black) in panels (a)–(c) in promil. (a) Glacial-interglacial transitions from benthic δ^{18}O ocean sediments as a proxy of global ice volume (Lisiecki and Raymo 2005) (note the inverse y-axis). (b) Variations in Asian summer monsoon intensity in the δ^{18}O record of the Hulu speleothem stack (Cheng *et al* 2016). (c) Stadial-interstadial transitions, also known as Dansgaard–Oeschger (DO) events, for the last glacial interval in ice core δ^{18}O from the North Greenland Ice Core Project (NGRIP Members 2004); the numbering of the DO events here follows Rousseau *et al* (2022). (d) Bond events 0–8 during the Holocene, shown in a North Atlantic ice drift index based on hematite-stained grains (Bond *et al* 2001).

driving of the ice ages at this time scale is unlikely (a) due to the very small amplitudes in solar irradiation associated with these eccentricity changes; and (b) with the fact that changes in the Solar System's orbital periodicities only occur on much longer time scales (Varadi *et al* 2003, Laskar *et al* 2004).

It has been suggested early on that the MPT is due to a transition of a nonlinear, oscillatory dynamical system forced by slow external forcing, e.g. by the slow increase in overall ice mass on the planet (Ghil and Childress 1987) or by the decrease in atmospheric CO_2 concentration (Saltzman and Maasch 1991). Several hypotheses as to the cause of the MPT are still under discussion (Chalk *et al* 2017) and a fairly extensive and annotated list is provided in Riechers *et al* (2021).

3.5. Stadial-interstadial cycles and DO events

During previous glacial intervals, abrupt climate transitions occurred at millennial time scales; these

DO events were first discovered in ice core records from the Greenland ice sheet (Oeschger *et al* 1984, Dansgaard 1987, Dansgaard *et al* 1993). The DO events between the cooler stadial and the warmer interstadial conditions are characterized by abrupt temperature increases of up 16 °C in high northern latitudes (Kindler *et al* 2014), within a few years (Steffensen *et al* 2008). In Greenland these temperature increases only last a few decades (Rasmussen *et al* 2014, Rousseau *et al* 2017) and are followed by gradual cooling over centuries to millennia, before a switch to more abrupt cooling leading back to stadial conditions, as illustrated in figure 3(c).

The millennial variability associated with the DO events is likely to have existed at least since 0.8 Ma, according to Rousseau *et al* (2022) and references therein. A complete fast-warming-and-slow-cooling cycle is also called a DO cycle (Alley 1998, Rousseau *et al* 2022).

In contrast to the glacial-interglacial cycles, the DO events are generally believed to be caused by self-sustained irregular oscillations within the climate system, generated by the interplay of sea ice, atmospheric dynamics, and the AMOC (Dokken *et al* 2013, Peltier and Vettoretti 2014, Vettoretti and Peltier 2016, Boers *et al* 2018). Freshwater discharges from the Laurentide ice sheets may have also played an important role. It has nevertheless been argued that the background climate conditions, sea levels and ice sheet heights, varying on much slower time scales, do determine to some extent the duration of the warmer episodes and the frequency of the abrupt transitions from colder to warmer conditions, as well as the duration of the warmer episodes during the glacial intervals (Zhang *et al* 2014, Boers *et al* 2018, Rousseau *et al* 2022).

The climate and ecosystem imprint of the DO events is global; it is assumed that the associated changes in AMOC strength led to episodes of gradual warming and cooling in Antarctica, during stadial and interstadial conditions, respectively, with temperature maxima in Antarctica shortly after the DO transitions in the North Atlantic (Svensson *et al* 2020). A common explanation for this coupling between the hemispheres, termed the bipolar seesaw, invokes a heat reservoir that convolves the signal originating from the North Atlantic on its way to Antarctica (Stocker and Johnsen 2003). This simple concept has been confirmed in the temperature reconstruction based on a well-resolved Antarctic ice core (EPICA Community Members 2006), although the atmospheric circulation may also be involved in the bipolar seesaw (Pedro *et al* 2018). In addition, the AMOC shifts have been argued to lead to changes in the meridional position of the Intertropical Convergence Zone (ITCZ), which directly affected the South American monsoon system, as seen in speleothem data (Mosblech *et al* 2012). In combination with displacements of the westerlies due to changes in North Atlantic sea-ice cover, the ITCZ shifts also led to marked shifts in the rainfall patterns of the Indian and East Asian monsoon systems (Cheng *et al* 2016), with implications for the carbon stock in the tropics (Bozbiyik *et al* 2011).

Given their relative abruptness and strong regional and global impact on climate and ecosystems, the DO events are considered as the archetype of abrupt climate changes and serve as a benchmark in testing our physical understanding of abrupt transitions in Earth system dynamics. Although the background climate today is very different from the last glacial, when DO events were frequently occurring, similar mechanisms may be triggered during the current anthropogenic heating of the Earth. For instance, the modern AMOC circulation is still vulnerable to changes in the ocean's surface density structure, which today is measurably perturbed by the warming (Johnson and Lyman 2020) and the intensification of the hydrological cycle (Durack *et al* 2012).

Note that, while many conceptual models have been proposed to explain the stadial-interstadial variability, faithful simulations of the characteristic series of past DO events in comprehensive climate models has only recently been achieved (Peltier and Vettoretti 2014, Vettoretti and Peltier 2016, Klockmann *et al* 2020).

3.6. Bond events and Bond cycles

During the Holocene, the North Atlantic experienced recurrent and sharp coolings that are commonly referred to as Bond events (Bond *et al* 1997, 2001). The nine Bond events of Bond *et al* (1992) are displayed in figure 3(d).

The most intensely studied events are those at 8.2 kyr, 5.9 kyr, and 4.2 kyr b2k, assumed to be related to changes in AMOC strength in response to ice discharge from the waning ice sheets of the Northern hemisphere, resulting freshening of the North Atlantic. For the 8.2 kyr b2k event, it has been suggested that the main source of freshwater stems from the collapse of the Laurentide Ice Sheet (Barber *et al* 1999). The event is mainly characterized by abrupt Northern-Hemisphere cooling, accompanied by drying in North Africa and Mesopotamia (Kobashi *et al* 2007) and disruptions of the Indian and East-Asian summer monsoons.

The 5.9 kyr b2k event is associated with the desertification of the previously *Green Sahara*. The collapse of this densely vegetated Sahara region to its current desert state is arguably the most important example of an abrupt state change of a coupled atmosphere–vegetation system (Brovkin *et al* 1998, Claussen *et al* 1998, Hales *et al* 2006). It is still a challenge to reproduce this transition of North African climate from relatively humid to persistently dry conditions in climate models, although at least conceptually, the relevant feedback mechanisms appear to have been relatively well understood for some time (Charney 1975, Charney *et al* 1975). Only recently have Hopcroft and

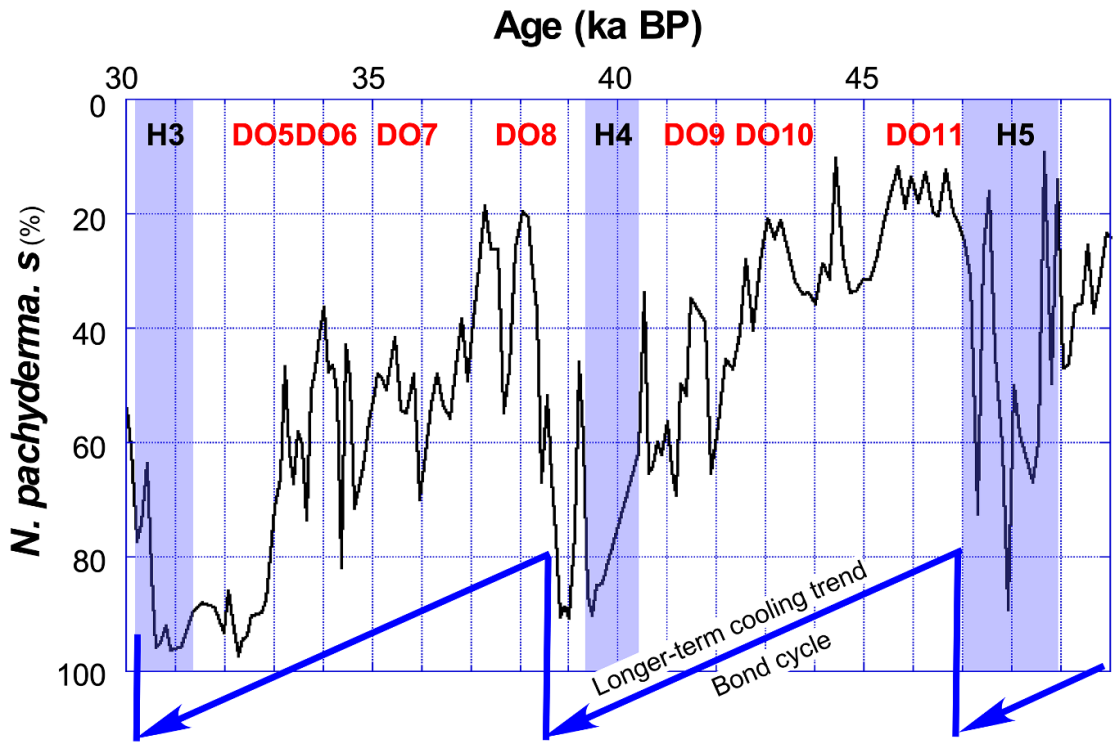

Figure 4. Synthetic description of two Bond cycles; 'DO' stands for a Dansgaard–Oeschger event and 'H' stands for a Heinrich event (Heinrich 1988, Ghil 1994). The solid black line shows the variations in the percentage of *Neogloboquadrina pachyderma* (s.), a planktonic foraminifera indicative of cold surface water, from DSDP 609 (Bond *et al* 1992); the solid blue line is the schematic representation of the two Bond cycles captured by the proxy record. The numbering of the Heinrich events follows Bond *et al* (1992), that of the DO events follows Rousseau *et al* (2022). Note that time runs from right to left here. Reproduced from Rousseau *et al* (2022). CC BY 4.0.

Valdes Hopcroft and Valdes (2021) shown that the abrupt Sahara desertification can be reproduced in a fairly detailed ESM with model parameters that are strongly constrained by using mid-Holocene climate proxy reconstructions.

For the 4.2 kyr event the records do not show an equally strong global cooling as for the 8.2 kyr event, but drying—in particular in North Africa, Mesopotamia, and the Asian monsoon domain—is evident (Gupta *et al* 2003). It has been speculated that the resulting droughts contributed to the collapse of the Akkadian empire in Mesopotamia (Gibbons 1993), as well as to that of the Old Kingdom in Egypt (Stanley *et al* 2003).

A connection between rapid events on the millennial time scale and more gradual shifts in overall climate has been proposed (Alley 1998, Rousseau *et al* 2022) and it is illustrated in figure 4. The figure plots so-called Bond cycles, as captured by a high-resolution proxy record. It shows a sequence of DO cycles composed of an abrupt warming that is followed by a slow return to glacial conditions, as discussed in section 3.5. Every Bond cycle contains several DO cycles and it is dominated by a long-term cooling trend that starts with a strong warming and ends with a stadial that includes a massive iceberg discharge into the North Atlantic; the Heinrich events (Heinrich 1988, Ghil 1994) are marked by the letter 'H' followed by a number assigned by Bond *et al* (1992).

It thus appears that somewhat irregular oscillations with a sawtooth-like appearance on two distinct millennial scales are embedded into each other like Russian dolls. The abrupt component of the sawtooth—whether DO event or Bond event—might, therewith, not be due to the kind of double-fold bifurcation shown in figure 2 and discussed in section 3.1 herein but to the kind of relaxation oscillations apparent in the FitzHugh–Nagumo model of DO cycles, as studied in section 3.3 of Riechers *et al* (2021).

Such a dual interpretation of available data on abrupt transitions is likewise possible in low-frequency atmospheric variability on the time scale of tens of days, as noted in Ghil and Robertson (2002). The transitions between blocked and zonal flow regimes (Weeks *et al* 1997) have been interpreted as either jumps between attractor basins of coexisting stable fixed points (Charney and DeVore 1979, Ghil and Childress 1987) or as slow phases of intraseasonal oscillations (Jin and Ghil 1990, Strong *et al* 1995).

The amount of observational data pertaining to atmospheric variability on these much shorter time scales vastly exceeds, in both amount and accuracy, the proxy records available for paleoclimate. Still, there is no widely agreed upon theory to decide

between the two dual points of view or some combination thereof in the better documented case of the shorter time scales either; see Hannachi *et al* (2017), Ghil *et al* (2018)and references therein.

4. Candidates for abrupt transitions under ongoing global warming

4.1. The Greenland and Antarctic ice sheets

The most important positive—and thus potentially destabilizing—feedback mechanism relevant for the dynamics of ice sheets is the melt-elevation feedback (Weertman 1961, Källén *et al* 1979, Ghil and Childress 1987, Levermann and Winkelmann 2016): an initial melting effectively reduces the ice sheet surface, which exposes it to relatively warmer temperatures due to the atmospheric lapse rate; in turn, this leads to enhanced melting, further height reductions, and so on. This idea goes back to Weertman (1961); see also section 11.2 and figure 11.10 in Ghil and Childress (1987). In fact, figure 1 in Levermann and Winkelmann (2016) resembles very much figure 11.10 in Ghil and Childress (1987).

A simplified, scalar version of the Weertman ice sheet model was coupled with a scalar EBM in Källén *et al* (1979), yielding oscillatory behavior with a time scale of 6–7 kyr for the waxing and waning of ice sheets, i.e. roughly the intervals between Heinrich ice rafting events; see Ghil (1994) and figure 4 herein. It stands to reason that a negative feedback on a shorter time scale, paired with a positive feedback like the ice-albedo one, could also lead to oscillatory, rather than bistable, behavior on the human time scales we are interested in most for the future. For instance, in Rombouts and Ghil (2015), the ice sheet equation à la (Weertman 1961) of the Källén *et al* (1979) model was replaced by a temperature-dependent vegetation equation, yielding oscillations with a periodicity of roughly 1 kyr, rather than the 6–7 kyr found in the original model and in the approximate spacing of the Heinrich events.

Still, there are important positive and negative feedbacks on shorter time scales as well, such as the positive one related to the albedo difference between white snow and gray ice (Box *et al* 2012): once the white upper snow and firn layers, which are usually a few tens of meters thick, are melted, the considerably darker bare ice is exposed (Ryan *et al* 2019), absorbing much more energy and thus further enhancing the melting. Moreover, once the firn layer has disappeared, meltwater runs off directly, rather than being refrozen inside the firn layer that it infiltrated. Additional positive feedbacks are related to snowline migration (Ryan *et al* 2019) and the thinning of outlet glaciers (Aschwanden *et al* 2019).

On the other hand, there also exist negative, and thus stabilizing feedbacks that mostly act via enhancing accumulation. Thus, the temperature-precipitation feedback introduced by Källén *et al* (1979), Ghil (1994) is based on the idea that accumulation will increase with rising temperatures and a more active hydrologic cycle. Moreover, at least for the Greenland ice sheet, it has been suggested that, with decreasing elevation, regional atmospheric circulation patterns may change in ways that increase accumulation (Hakuba *et al* 2012).

Greenland has lost substantial amounts of ice in the course of the last century (Kjeldsen *et al* 2015, Mouginot *et al* 2019). The Greenland ice sheet holds the equivalent of 7 m of global sea level (Gregory *et al* 2004, Enderlin *et al* 2014) and comprehensive model simulations suggest that, under the RCP8.5 emission scenario, it would take roughly 800 years for the ice sheet to melt down entirely (Aschwanden *et al* 2019).

The stability of the Greenland ice sheet depends crucially on the relative contributions of the positive and negative feedbacks mentioned above. Robinson *et al* (2012), using a model of intermediate complexity, suggested that there exists a critical temperature threshold beyond which complete melting would be inevitable, and that there would be pronounced hysteresis when reducing atmospheric temperatures. These authors estimated the corresponding temperature threshold to lie within the range of 1.1 °C–2.3 °C with a best estimate of 1.8 °C global mean temperature anomaly above pre-industrial levels. More recent coupled model studies suggest, however, that there might be additional stable states at intermediate ice sheet heights. Still, the mass loss accompanying the transition from the current ice sheet state to the next, intermediate stable state would be dramatic and practically irreversible (Gregory *et al* 2020).

The Antarctic ice sheet has lost mass at a rapidly increasing rate in recent decades (Rignot *et al* 2019), mainly due to West Antarctica's outlet glaciers, which lead into the Amundsen Sea, and their accelerating flow (Shepherd *et al* 2018). The key destabilizing feedback in this case is the marine ice sheet instability. Sea level lies above the bedrock of the West Antarctic ice sheet, whose negative slope towards the continent's interior—called a reverse slope—can lead to rapid motion of the ice sheet's grounding line and thus destabilize it (Schoof 2007).

4.2. The AMOC

The AMOC is the Atlantic Ocean component of the global thermohaline circulation, transporting water masses from the southern to the northern Atlantic Ocean near the surface, and from north to south in the ocean's deep layers (Richardson 2008). Early studies using conceptual models have suggested that the AMOC is bistable (Stommel 1961, Bryan 1986, Stocker and Wright 1991, Quon and Ghil 1992, Dijkstra and Ghil 2005). The AMOC is assumed to be primarily driven by the sinking motion of salty and thus heavy water masses in the North Atlantic, although wind-driven changes in the Antarctic Circumpolar Current are also playing a role (Cessi 2019,

Ghil and Lucarini 2020). The main nonlinear mechanism underlying the AMOC's bistability is the salt-advection feedback: the stronger the circulation, the more salty water masses are brought to the North Atlantic, in turn amplifying the circulation.

Paleoclimate proxy records indeed suggest that the DO cycles of past glacial intervals were accompanied by switches between the AMOC's current strong mode and a substantially weaker one (Stocker 2000, Rahmstorf 2002, Henry *et al* 2016, Boers *et al* 2018). Speleothem records, in particular, suggest substantial impacts of the AMOC transitions on global climate variability (Wang *et al* 2008, Kanner *et al* 2012, Mosblech *et al* 2012).

Several experiments with EMICs have confirmed the AMOC's bistability (Manabe and Stouffer 1988, Stocker and Wright 1991, Knutti and Stocker 2002, Rahmstorf *et al* 2005, Hawkins *et al* 2011). Although more comprehensive GCMs have had difficulties in reproducing the AMOC's bistability (Liu *et al* 2014, 2017), some comprehensive models do exhibit it (Ferreira *et al* 2011, 2018), and a recent high-resolution, eddy-permitting model has in fact reproduced the bistability (Jackson and Wood 2018). Such high-resolution models also suggest severe impacts if the AMOC were to transition to its weak circulation mode in response to global warming, entraining in turn pronounced temperature and rainfall reduction in the higher northern latitudes, and strong disturbances of the tropical monsoon systems (Jackson *et al* 2015).

Although the AMOC is still in its strong mode, proxy data suggest that it may well be at its weakest in the last 1500 years (Thornalley *et al* 2018, Caesar *et al* 2021). While comprehensive model projections of its response to further rising temperatures in the coming decades to centuries generally agree that the AMOC will continue to slow down, considerable uncertainties remain on the actual amount of reduction and the likelihood of an abrupt transition to the weak circulation mode (Stocker and Schmittner 1997, Hu *et al* 2013, IPCC 2021a).

The reasons for the observed AMOC weakening are still being debated, but three processes conspire to slow down the AMOC in the future. First, a warming of the SST field of the North Atlantic reduces surface density and therefore the sinking to deeper ocean levels. Second, more warming in the extratropics leads to more evaporation and an enhanced meridional transport of moisture in the atmosphere. As a result, precipitation increases in the mid-to-high latitudes, which reduces salinity and surface density, a feature that is already observed globally (Durack *et al* 2012). Third, enhanced freshwater inflow caused by increased Greenland ice sheet meltwater runoff, Arctic sea-ice melting, and an overall enhanced hydrological cycle at higher atmospheric temperatures might have started to play an important role as well.

Evidence for critical slowing down in observation-based AMOC fingerprints from SSTs and surface salinity data—in the sense described in section 2.4 herein—suggests that the recent AMOC slowing is not just a linear response to the warming atmosphere, but may instead be associated with a dynamical loss of stability; i.e. a shift of the AMOC toward the bifurcation point at which an abrupt transition to the weak circulation mode may occur (Boers 2021). The key question remains whether the AMOC shows a bifurcation depending on the warming level and its rate, and would hence potentially exhibit irreversibility (Stocker and Schmittner 1997).

An alternative, or at least complementary, explanation of the AMOC's slowing down could be the kind of multidecadal oscillation found in some intermediate complexity (Chen and Ghil 1996, Ghil 2001) to high-end models (DelSole *et al* 2011), although this explanation is still being contested (Mann *et al* 2020). Such an oscillatory, rather than bistable, AMOC behavior is illustrated in figure 6. The periodicity of the limit cycle arising from the Hopf bifurcation in figure 6(b) is of 40–50 years and its peak-to-peak amplitude in meridional overturning is roughly 3 Sv. Clearly such an oscillation could explain—or at least contribute, in its decreasing phase—to the observed AMOC weakening.

4.3. Tropical monsoon systems

Paleoclimatic variability in the three major monsoon systems of Southern and Eastern Asia, Western Africa, and South America are mostly recorded in speleothem records from the affected regions; see figure 3(b). All three depend strongly on the latitudinal position of the ITCZ, which is in turn affected by the strength of the AMOC (Stouffer *et al* 2006). In particular for the West African Monsoon, a shift to permanently drier conditions in response to an AMOC collapse has been suggested. For the Indian and East Asian Summer Monsoon, shifts in rainfall amounts synchronous with the stadial-interstadial cycles (Cheng *et al* 2016), but also in response to the Bond events (Goswami *et al* 2018) have been identified.

Speleothem proxy records suggest that during the last glacial, the South American monsoon was stronger during stadials, with weaker AMOC and thus a southward shifted ITCZ (Kanner *et al* 2012, Mosblech *et al* 2012). On the other hand, comprehensive model simulations indicate an overall reduction of mean annual rainfall in large parts of tropical South America and a southeastward shift of the core monsoon region of South America (Jackson *et al* 2015). Dry-season rainfall in tropical South America, though, is projected to increase (Parsons *et al* 2014), due to the ITCZ's overall southward shift.

Compared to other potentially bistable Earth system components, like the ones discussed thus far,

there is relatively little literature, such as (Levermann *et al* 2009), on the mechanisms and feedbacks that might lead to an abrupt monsoon shift in response to anthropogenic forcing. Rising temperatures and changing humidity or aerosol concentrations have been mentioned as contributing factors. Given the ecological and socioeconomic importance of the tropical monsoon systems, we stress their potentially abrupt response to global warming and other human influences as an important subject of future research.

4.4. The Amazon rainforest

It has been suggested that for intermediate rainfall regimes, the Amazon vegetation system can be either in a rainforest or in a savanna state (Hirota *et al* 2011), in a manner reminiscent of figure 2 herein. As noted above, rainfall in tropical South America depends crucially on the latitudinal position of the ITCZ, which in turn depends on SSTs in the tropical Atlantic ocean (Robertson *et al* 2003, Harris *et al* 2008). Indeed, two of the most severe droughts during the last century, in 2005 and 2010, have been attributed to anomalously warm SSTs in the northern tropical Atlantic (Marengo *et al* 2011, Ciemer *et al* 2020).

Models suggest that reducing Northern-Hemisphere atmospheric aerosol concentrations may lead to further increases in drought frequency (Cox *et al* 2008). A possible collapse of the AMOC would, via the associated increases in dry-season rainfall in tropical South America, lead to a stabilization of the Amazon rainforest (Ciemer *et al* 2021, Good *et al* 2021), although this issue is far from settled.

In addition to the impacts of potentially changing rainfall patterns and the direct response of the vegetation system to higher temperatures, the Amazon rainforest is threatened by direct deforestation and land-use changes (Betts *et al* 2008, Davidson *et al* 2012). Ongoing forest degradation may already have led to an observable increase in dry-season length (Fu *et al* 2013, Marengo *et al* 2018), imposing further stress on parts of the rainforest that are intact so far.

Model simulations vary greatly in their projections of the rainfall response to Amazon deforestation, with reductions up to 40% for complete removal of the rainforest (Spracklen and Garcia-Carreras 2015). A positive feedback between latent heating over the Amazon and atmospheric low-level circulation is likely to enhance the strength of moisture flux into tropical South America (Rodwell and Hoskins 2001). Ongoing deforestation could—via the resulting reduction in moisture recycling between atmosphere and land surface—reduce the overall moisture content to a degree at which the latent-heat feedback might break down, causing abrupt rainfall decline (Boers *et al* 2017). Critical slowing down has recently been discovered in satellite-derived vegetation indices, suggesting a strong loss of Amazon rainforest resilience since the early 2000s (Boulton *et al* 2022, Smith *et al* 2022).

4.5. Abrupt climate transitions and the model hierarchy

It has been mentioned already in the section 1 that, overall, comprehensive climate and ESMs have difficulties in reproducing abrupt climate transitions, possibly because of these models' being excessively stable (Valdes 2011) or because of being overfitted to current climate conditions (Ghil and Lucarini 2020). In particular, it has been noted in section 4.2 that high-end models may exhibit a too stable AMOC (Liu *et al* 2017); a state of affairs that is, in all likelihood, related to biases in the salinity field and the freshwater export (Dijkstra 2007, Mecking *et al* 2017a).

As likewise noted in section 4.2, though, recent simulations at eddy-permitting resolution have in fact identified a bistable AMOC (Jackson and Wood 2018). More generally, a systematic search has revealed 37 abrupt regional climate transitions in the projections of the fifth phase of the Coupled Model Intercomparison Project (CMIP5) (Drijfhout *et al* 2015). Moreover, in the course of the last years, DO-like oscillations have been produced in a number of comprehensive models (Peltier and Vettoretti 2014, Vettoretti and Peltier 2016, Klockmann *et al* 2020).

In a similar vein, earlier work based on conceptual models had proposed underlying mechanisms for bistability of the Sahel-and-Sahara arid belt (Charney 1975, Brovkin *et al* 1998). But, as noted already in section 3.6, it is only quite recently that a comprehensive coupled atmosphere-vegetation model has benefited from tuning to paleoclimate proxy data from the 4–6 kyr b2k time interval to reproduce the desertification of the Green Sahara (Hopcroft and Valdes 2021).

This kind of development suggests that persisting disagreements among different models regarding the future evolution of the Amazon rainforest in response to anthropogenic heating and deforestation (Betts *et al* 2004, Cox *et al* 2004, Good *et al* 2013, Huntingford *et al* 2013, Drijfhout *et al* 2015) could be settled in the not too distant future. Moreover, it has recently been shown that those models that have more realistic land-atmosphere interactions when compared to observations also give relatively robust projections for future rainfall patterns in the Amazon region (Baker *et al* 2021).

The concept of a hierarchy of models (Schneider and Dickinson 1974, Ghil 2001, Held 2005), introduced already in section 1, can be very helpful in reaching more definitive conclusions about the existence, nature, causes and robustness of abrupt transitions in the global Earth system or components thereof (Lenton *et al* 2008, Ashwin *et al* 2012, Ghil and Lucarini 2020). Successively more complex bifurcations (Ghil and Childress 1987, Ghil 2001)—outlined

here in section 2—can be pursued most easily for relatively simple or intermediate-complexity models of the Earth system or of its components. Still, such bifurcations have been shown recently to manifest themselves in some of the more detailed climate and ESMs, as discussed in this subsection. To the extent that the first few branchings in a bifurcation tree can be shown to persist as the models become more sophisticated and detailed, our confidence in their actual presence in the system itself will increase.

It is imperative, moreover, to improve the data base against which models at each step of the hierarchy can be compared (Bagniewski *et al* 2021). A fine example of such a three-way comparison of two models of unequal complexity with observations and with the inferred bifurcation structure is given by Dijkstra (2007). This specific example shows that, when a simpler model and a more detailed one disagree, it is not always the former that is wrong; that is, adding details does not always add realism. Inspired by the work of Stommel (1961), a series of papers using AMOC models from simple to intermediate and beyond, had obtained bistability of the meridional-overturning circulation, especially in situations mimicking the Atlantic Ocean; see Dijkstra (2005), Dijkstra and Ghil (2005) for a review. High-end ocean models used in CMIP3—on which the conclusions of the IPCC's Fourth Assessment Report (IPCC 2007) were based—obtained, however, results that contradicted this bistability. As shown by Dijkstra (2007), Ghil (2015), observations of the evaporation-minus-precipitation fluxes over the Atlantic, between the southern tips of Greenland and Africa, agree better with the simpler models than with those used in IPCC (2007); and it is this better agreement that supports the bistability results of the former, simpler models. These analyses have motivated and inspired in-depth analyses of the stability profile of the AMOC for more recent model generations and may have helped improve the AMOC representation in these models; for example, the eddy-permitting CMIP6 model HadGEM3-GC2 does exhibit a bi-stable AMOC, with associated hysteresis (Mecking *et al* 2016, 2017b, Jackson and Wood 2018). Further IPCC-class models appear to be on their way of reproducing a bistable AMOC.

5. Concluding remarks and broader implications

5.1. Scientific summary

The possibility of abrupt transitions in the Earth system or parts thereof, subject to a gradual rise of greenhouse gas and aerosol levels, adds a great deal of uncertainty to an already rather uncertain future for humanity's life on this planet. In section 2, we have briefly presented dynamical system theory—first in the presence of constant and then of time-dependent forcing—as an appropriate general framework for the study of abrupt transitions and the mechanism that might cause them; see, in particular, figure 2.

In section 3, we have summarized some of the existing evidence for such abrupt transitions on different time scales in the past; see again figures 3 and 4. Section 4 was dedicated to a summary of where we stand in the study of some of the Earth system components sketched in figure 5 as being exposed to tipping. More specifically, we have considered both bistability, as in figure 2, and Hopf bifurcation, as in figure 6, as nonlinear mechanisms that can induce an abrupt transition in a paleoclimatic system's behavior.

The overall conclusions are

(a) In the context of time-dependent forcing—both anthropogenic and natural—various types of tipping (Ghil 2001, Ashwin *et al* 2012) provide important and frequently encountered mechanisms for abrupt transitions.
(b) Paleoclimatic records testify to the presence of abrupt transitions on several time scales.
(c) Linking the observational evidence to the theory of non-autonomous and random dynamical systems is an emerging and valuable road to better understanding of such transitions in the past and to their prediction in the future.

There are many questions that we did not address or approaches that we did not cover, for lack of space. Some of these are listed below:

(a) uncertainty quantification in predicting abrupt transitions (Boettiger and Hastings 2012);
(b) applying necessary and sufficient conditions for the inference of causes to abrupt transitions found in paleo-records (Hannart *et al* 2016);
(c) applying data assimilation and systematic parameter estimation to improve nonlinear paleo-models capable of abrupt transitions (Roques *et al* 2014, Hopcroft and Valdes 2021).

5.2. Discussion of broader issues

Aside from these scientific points, it is clearly necessary to raise the level of interest of the broader community of stakeholders in abrupt transitions and in their disproportionately large socio-economic impacts. Three reasons stand out for doing so.

First, a broad consensus in the scientific community regarding tipping points and related instabilities is still lacking. While many paleoclimatic records exhibit numerous instances of rapid and abrupt changes, it is not clear whether current and future conditions of the climate system, particularly under anthropogenic forcing, would increase or decrease the stability of the tipping elements discussed so far. It is also not known whether new tipping elements that have no paleo-analogue could evolve and thus lead to true 'surprises' in the climate system. This lack of broad scientific consensus can result in a very fuzzy public perception of tipping points. Either relegating

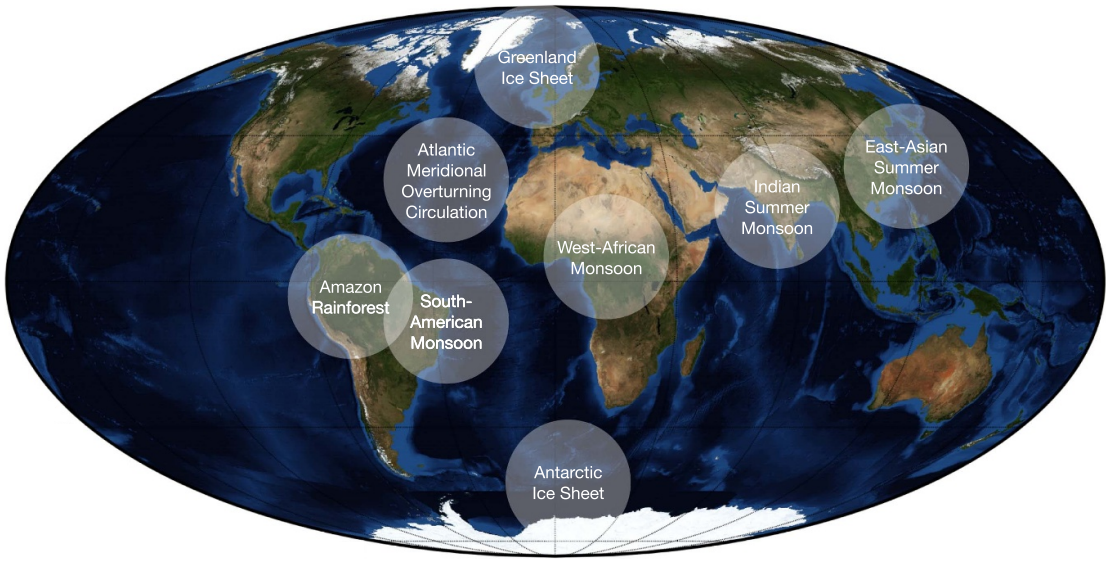

Figure 5. Geographical map showing important components of the Earth system that may respond abruptly to ongoing anthropogenic forcing.

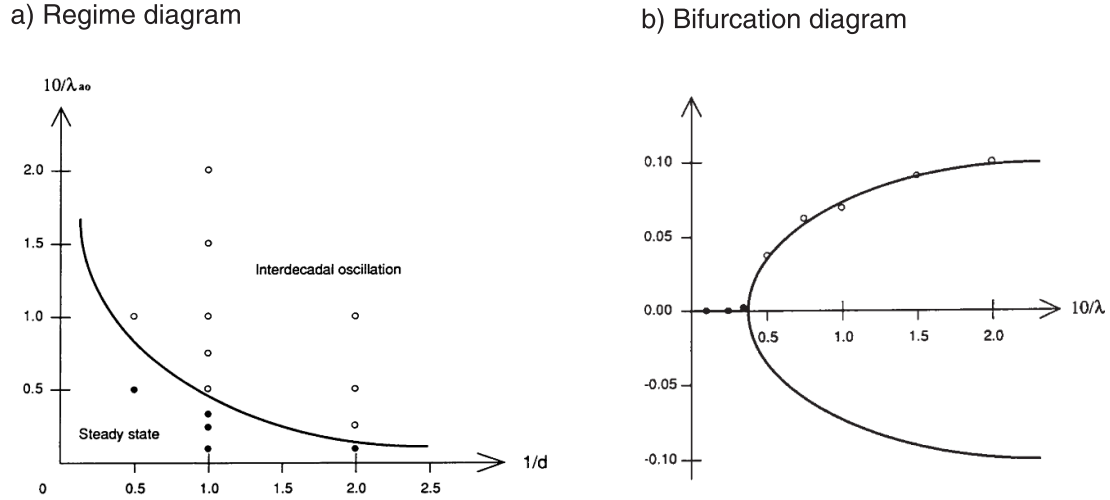

Figure 6. Dependence of AMOC solutions on two parameters in a hybrid coupled model, with a fully three-dimensional ocean model and a two-dimensional atmospheric model of energy-balance type. The two parameters are the atmosphere–ocean coupling coefficient λ_{ao} and the atmospheric thermal diffusion coefficient d. (a) Schematic regime diagram. The full circles stand for the model's stable steady states, the open circles for stable limit cycles, and the solid curve is the estimated neutral stability curve between the former and the latter. (b) Hopf bifurcation curve at fixed $d = 1.0$ and varying λ_{ao}; this curve was obtained by fitting a parabola to the model's numerical simulation results, shown as full and open circles. Reproduced from Chen and Ghil (1996). © American Meteorological Society. Used with permission.

tipping points to the world of mathematical peculiarities or elevating them to the level of an inevitable catastrophe is not useful for stimulating mitigation and adaptation and can, to the contrary, induce indifference and lack of appropriate action.

Building scientific consensus, and being explicit about where is has not yet been achieved, is the core task of the IPCC. The preparation of an IPCC assessment report is essentially a consensus-building process. It forces the scientific community to assess the current state of knowledge on a specific issue, formulate a consensus where possible, map out the uncertainties, debate the confidence level, and point out where consensus cannot be achieved. A point in case is the sign of the net water vapor feedback in the climate system, for which over successive assessment cycles a robust scientific consensus was found and communicated: the water vapor feedback is positive (IPCC 2021b).

The topic of abrupt transitions, or tipping points, in the climate and Earth system has never undergone this process of community scrutiny and, therefore, we would advocate the commissioning of a Special Report on Tipping Points in the forthcoming seventh assessment cycle of the IPCC. From past experience, the commissioning of such a report (Ghil

and Lucarini 2020) and the ensuing community activity accelerate considerably scientific progress on the topic of choice. More broadly, it will stimulate the integration of the concepts and tools of dynamical system theory into the thinking habits of the ESM community.

Such an integration would have to rely on the use (a) of reduced-order models in the analysis of various types of observational data sets and the exploration of ESM behavior (Kondrashov *et al* 2005, Kravtsov *et al* 2009); and (b) of advanced numerical methods in the study of the bifurcation trees of intermediate and high-end models. Continuation methods for the study of multiple branches of solutions in such models have been greatly improved and applied successfully to models with an order of millions of grid-point variables (Simonnet *et al* 2009, Dijkstra *et al* 2014).

Second, more robust science on tipping points calls for a three-pronged approach: (a) more targeted observations of critical elements such as the AMOC or ice streams in Antarctica; (b) much improved climate models; and (c) a more systematic way of using the latter. The present generation of models still has problems in representing highly non-linear processes at both small and large scales, such as atmosphere–ocean interactions that determine deep-water formation and hence AMOC or ice-sheet and ocean processes that determine the fate of ice sheets under current anthropogenic heating. Hence improving the representation of individual processes and increasing model resolution substantially is of as much importance as ever before (Palmer and Stevens 2019). Taking into account the difference in characteristic scales in the atmosphere vs. the ocean, cloud-resolving scales in the one and truly eddy-resolving scales in the other would make a big difference in understanding and hence prediction of key processes that may bring us closer to reliably representing tipping elements in models.

But in pursuing the study of tipping, it is of utmost importance to realize that the performance of a given model, on whatever rung of the modeling hierarchy, has to be seen as a possibly discontinuous function of its parameters and not studied just for a single, given value of each parameter. It is now well understood in numerical weather prediction that, for best results, a model has to be run for an ensemble of initial conditions and not just for a single initial state, no matter how optimally chosen. In the same way, a climate or ESM has to sweep a whole region of its parameter space, not just use a single set of values, no matter how well that one point in parameter space was tuned to available data. The proximity of a tipping point can depend in surprising ways on unsuspected, secondary parameters (Zaliapin and Ghil 2010). The choice of the parameters and of the range one has to sweep can and should be chosen and optimized by using simpler and more efficient models than the final one.

Third, economic models are in their infancy regarding physical, technological, and socio-economic disruptions, a hallmark of tipping elements in the Earth System. The generalized equilibrium models that dominate neoclassical macroeconomics are not well suited to inform us about the economic and financial consequences of abrupt changes in climate and the environment. Policymakers and socio-economic stakeholders lack, therefore, the essential scientific information on the risks and implications of crossing a threshold in factors extrinsic to the macroeconomic models in use. Building on an emerging consensus of the physical science basis regarding tipping points—such as the one that would be achieved in the course of an IPCC assessment cycle—could be an important step in a more realistic engagement between open-minded economists and climate scientists (Barnett *et al* 2020, Ghil 2020, 2022, Lackner *et al* 2022, Ogutu *et al* 2022).

Data availability statement

No new data were created or analyzed in this study.

Acknowledgments

It is a pleasure to thank Denis-Didier Rousseau for figure 4, as well as for the careful reading of an earlier version of the paper and several judicious comments. Two anonymous referees have provided constructive and useful criticism and suggestions. This is TiPES Contribution #170; the Tipping Points in the Earth System (TiPES) project has received funding from the European Union's Horizon 2020 research and innovation programme under Grant Agreement No. 820970. This project has received further funding from the European Union's Horizon 2020 Research and Innovation Programme under the Marie Skłodowska–Curie Grant Agreement No. 956170. N B acknowledges funding by the Volkswagen Foundation. T F S acknowledges support through Project No. 200492 of the Swiss National Science Foundation.

ORCID iD

Niklas Boers https://orcid.org/0000-0002-1239-9034

References

Alley R B 1998 Icing the North Atlantic *Nature* **392** 335–7

Almazroui M *et al* 2021 Assessment of CMIP6 performance and projected temperature and precipitation changes over South America *Earth Syst. Environ.* **5** 155–83

Arnold V I 2012 *Geometrical Methods in the Theory of Ordinary Differential Equations* 1st Russian edn (New York: Springer Science & Business Media) p 1978

Arnold V I, Kozlov V V and Neishtadt A I 2007 *Mathematical Aspects of Classical and Celestial Mechanics* vol 3 (Berlin: Springer Science & Business Media)

Arrhenius S 1896 On the influence of carbonic acid in the air upon the temperature of the ground *London, Edinburgh Dublin Phil. Mag. J. Sci.* **41** 237–76
Aschwanden A, Fahnestock M A, Truffer M, Brinkerhoff D J, Hock R, Khroulev C, Mottram R and Abbas Khan S 2019 Contribution of the Greenland ice sheet to sea level over the next millennium *Sci. Adv.* **5** eaav9396
Ashwin P, Wieczorek S, Vitolo R and Cox P 2012 Tipping points in open systems: bifurcation, noise-induced and rate-dependent examples in the climate system *Phil. Trans. R. Soc.* A **370** 1166–84
Bagniewski W, Ghil M and Rousseau D D 2021 Automatic detection of abrupt transitions in paleoclimate records *Chaos* **31** 113129
Baker J C, Garcia-Carreras L, Buermann W, Castilho De Souza D, Marsham J H, Kubota P Y, Gloor M, Coelho C A and Spracklen D V 2021 Robust Amazon precipitation projections in climate models that capture realistic land-atmosphere interactions *Environ. Res. Lett.* **16** 074002
Barber D C *et al* 1999 Forcing of the cold event of 8,200 years ago by catastrophic drainage of Laurentide lakes *Nature* **400** 344–8
Barnett M, Brock W and Hansen L P 2020 Pricing uncertainty induced by climate change *Rev. Financ. Stud.* **33** 1024–66
Benzi R, Parisi G, Sutera A and Vulpiani A 1982 Stochastic resonance in climatic change *Tellus* **34** 10–15
Benzi R, Sutera A and Vulpiani A 1981 The mechanism of stochastic resonance *J. Phys. A: Math. Gen.* **14** L453
Berger A 1978 Long term variations of daily insolation and Quaternary climate change *J. Atmos. Sci.* **35** 2362–7
Betts R A, Cox P M, Collins M, Harris P P, Huntingford C and Jones C D 2004 The role of ecosystem-atmosphere interactions in simulated Amazonian precipitation decrease and forest dieback under global climate warming *Theor. Appl. Climatol.* **78** 157–75
Betts R A, Malhi Y and Roberts J T 2008 The future of the Amazon: new perspectives from climate, ecosystem and social sciences *Phil. Trans. R. Soc.* B **363** 1729–35
Bódai T and Tél T 2012 Annual variability in a conceptual climate model: snapshot attractors, hysteresis in extreme events and climate sensitivity *Chaos* **22** 023110
Boers N 2018 Early-warning signals for Dansgaard–Oeschger events in a high-resolution ice core record *Nat. Commun.* **9** 2556
Boers N 2021 Observation-based early-warning signals for a collapse of the Atlantic Meridional Overturning Circulation *Nat. Clim. Change* **11** 680–8
Boers N, Ghil M and Rousseau D-D 2018 Ocean circulation, ice shelf and sea ice interactions explain Dansgaard–Oeschger cycles *Proc. Natl Acad. Sci.* **115** E11005–14
Boers N, Marwan N, Barbosa H M J and Kurths J 2017 A deforestation-induced tipping point for the South American monsoon system *Sci. Rep.* **7** 41489
Boers N and Rypdal M 2021 Critical slowing down suggests that the western Greenland ice sheet is close to a tipping point *Proc. Natl Acad. Sci. USA* **118** e2024192118
Boettiger C and Hastings A 2012 Quantifying limits to detection of early warning for critical transitions *J. R. Soc. Interface* **9** 2527–39
Boettner C and Boers N 2022 Critical slowing down in dynamical systems driven by non-stationary correlated noise *Phys. Rev. Res.* **4** 013230
Boettner C, Klinghammer G, Boers N, Westerhold T and Marwan N 2021 Early-warning signals for Cenozoic climate transitions *Quat. Sci. Rev.* **270** 107177
Bond G *et al* 1992 Evidence for massive discharges of icebergs into the North Atlantic ocean during the last glacial period *Nature* **360** 245–9
Bond G, Kromer B, Beer J, Muscheler R, Evans M N, Showers W, Hoffmann S, Lotti-Bond R, Hajdas I and Bonani G 2001 Persistent solar influence on North Atlantic climate during the Holocene *Science* **294** 2130–6
Bond G, Showers W, Cheseby M, Lotti R, Almasi P, DeMenocal P, Priore P, Cullen H, Hajdas I and Bonani G 1997 A pervasive millennial-scale cycle in the North Atlantic Holocene and glacial climates *Science* **278** 1257–66
Boulton C, Lenton T and Boers N 2022 Pronounced loss of Amazon rainforest resilience since the early 2000s *Nat. Clim. Change* **12** 271–8
Box J E, Fettweis X, Stroeve J C, Tedesco M, Hall D K and Steffen K 2012 Greenland ice sheet albedo feedback: thermodynamics and atmospheric drivers *Cryosphere* **6** 821–39
Boysen L R *et al* 2020 Global climate response to idealized deforestation in CMIP6 models *Biogeosciences* **17** 5615–38
Bozbiyik A, Steinacher M, Joos F, Stocker T F and Menviel L 2011 Fingerprints of changes in the terrestrial carbon cycle in response to large reorganizations in ocean circulation *Clim. Past* **7** 319–38
Broecker W S and van Donk J 1970 Insolation changes, ice volumes and the δ^{18}O record in deep-sea cores *Rev. Geophys.* **8** 169–98
Brovkin V *et al* 2021 Past abrupt changes, tipping points and cascading impacts in the Earth system *Nat. Geosci.* **14** 550–8
Brovkin V, Claussen M, Petoukhov V and Ganopolski A 1998 On the stability of the atmosphere-vegetation system in the Sahara/Sahel region *J. Geophys. Res.* **103** 31613–24
Bryan F 1986 High-latitude salinity effects and interhemispheric thermohaline circulations *Nature* **323** 301–4
Budyko M I 1969 The effect of solar radiation variations on the climate of the Earth *Tellus* **21** 611–9
Bury T M, Bauch C T and Anand M 2020 Detecting and distinguishing tipping points using spectral early warning signals *J. R. Soc. Interface* **17** 20200482
Caesar L, Mccarthy G D, Thornalley D J R, Cahill N and Rahmstorf S 2021 Current Atlantic Meridional Overturning Circulation weakest in last millennium *Nat. Geosci.* **14** 118–21
Carpenter S R and Brock W A 2006 Rising variance: a leading indicator of ecological transition *Ecol. Lett.* **9** 311–8
Cessi P 2019 The global overturning circulation *Annu. Rev. Mar. Sci.* **11** 249–70
Chalk T B *et al* 2017 Causes of ice age intensification across the mid-Pleistocene transition *Proc. Natl Acad. Sci. USA* **114** 13114–9
Charney J G, Arakawa A, Baker D J, Bolin B, Dickinson R E, Goody R E, Leith C E, Stommel H M and Wunsch C I 1979 *Report of an Ad-Hoc Group on Carbon Dioxide and Climate. Technical Report* (Climate Research Board, National Research Council)
Charney J G and DeVore J G 1979 Multiple flow equilibria in the atmosphere and blocking *J. Atmos. Sci.* **36** 1205–16
Charney J 1975 Dynamics of deserts and drought in the Sahel *Q. J. R. Meteorol. Soc.* **101** 193–202
Charney J, Stone P H and Quirk W J 1975 Drought in the Sahara: a biogeophysical feedback mechanism *Science* **187** 434–5
Chekroun M D, Ghil M and Neelin J D 2018 Pullback attractor crisis in a delay differential ENSO model *Advances in Nonlinear Geosciences* ed A A Tsonis (Cham: Springer Science & Business Media) pp 1–33
Chekroun M D, Simonnet E and Ghil M 2011 Stochastic climate dynamics: random attractors and time-dependent invariant measures *Physica* D **240** 1685–700
Chen F and Ghil M 1996 Interdecadal variability in a hybrid coupled ocean-atmosphere model *J. Phys. Oceanogr.* **26** 1561–78
Cheng H *et al* 2016 The Asian monsoon over the past 640,000 years and ice age terminations *Nature* **534** 640–6
Ciemer C, Rehm L, Kurths J, Donner R V, Winkelmann R and Boers N 2020 An early-warning indicator for Amazon droughts exclusively based on tropical Atlantic sea surface temperatures *Environ. Res. Lett.* **15** 094087
Ciemer C, Winkelmann R, Kurths J and Boers N 2021 Impact of an AMOC weakening on the stability of the southern Amazon rainforest *Eur. Phys. J. Spec. Top.* **230** 3065–73

Claussen M *et al* 2002 Earth system models of intermediate complexity: closing the gap in the spectrum of climate system models *Clim. Dyn.* **18** 579–86
Claussen M, Brovkin V, Ganopolski A, Kubatzki C and Petoukhov V 1998 Modelling global terrestrial vegetation-climate interaction *Phil. Trans. R. Soc.* B **353** 53–63
Cox P M, Betts R A, Collins M, Harris P P, Huntingford C and Jones C D 2004 Amazonian forest dieback under climate-carbon cycle projections for the 21st century *Theor. Appl. Climatol.* **78** 137–56
Cox P M, Harris P P, Huntingford C, Betts R A, Collins M, Jones C D, Jupp T E, Marengo J A and Nobre C A 2008 Increasing risk of Amazonian drought due to decreasing aerosol pollution *Nature* **453** 212–5
Crucifix M 2018 Pleistocene glaciations *Climate Changes in the Holocene: Impacts and Human Adaptation* (Boca Raton, FL: CRC Press)
Dakos V, Scheffer M, van Nes E H, Brovkin V, Petoukhov V and Held H 2008 Slowing down as an early warning signal for abrupt climate change *Proc. Natl Acad. Sci. USA* **105** 14308–12
Dansgaard W 1987 Ice core evidence of abrupt climatic changes *Abrupt Climatic Change 1985* (Dordrecht: Springer) pp 223–33
Dansgaard W *et al* 1993 Evidence for general instability of past climate from a 250-kyr ice-core record *Nature* **364** 218–20
Davidson E A *et al* 2012 The Amazon basin in transition *Nature* **481** 321–8
DelSole T, Tippett M K and Shukla J 2011 A significant component of unforced multidecadal variability in the recent acceleration of global warming *J. Clim.* **24** 909–26
Dijkstra H A 2005 *Nonlinear Physical Oceanography: A Dynamical Systems Approach to the Large Scale Ocean Circulation and El Niño* 2nd edn (Berlin: Springer Science+Business Media)
Dijkstra H A 2007 Characterization of the multiple equilibria regime in a global ocean model *Tellus* A **59** 695–705
Dijkstra H A *et al* 2014 Numerical bifurcation methods and their application to fluid dynamics: analysis beyond simulation *Commun. Comput. Phys.* **15** 1–45
Dijkstra H A and Ghil M 2005 Low-frequency variability of the large-scale ocean circulation: a dynamical systems approach *Rev. Geophys.* **43** RG3002
Dokken T M, Nisancioglu K H, Li C, Battisti D S and Kissel C 2013 Dansgaard–Oeschger cycles: interactions between ocean and sea ice intrinsic to the Nordic seas *Paleoceanography* **28** 491–502
Drijfhout S, Bathiany S, Beaulieu C, Brovkin V, Claussen M, Huntingford C, Scheffer M, Sgubin G and Swingedouw D 2015 Catalogue of abrupt shifts in Intergovernmental Panel on Climate Change climate models *Proc. Natl Acad. Sci.* **112** E5777–86
Durack P J, Wijffels S E and Matear R J 2012 Ocean salinities reveal strong global water cycle intensification during 1950 to 2000 *Science* **336** 455–8
Eckmann J-P 1981 Roads to turbulence in dissipative dynamical systems *Rev. Mod. Phys.* **53** 643–54
Enderlin E M, Howat I M, Jeong S, Noh M J, van Angelen J H and van den Broeke M R 2014 An improved mass budget for the Greenland ice sheet *Geophys. Res. Lett.* **41** 866–72
EPICA Community Members 2006 One-to-one coupling of glacial climate variability in Greenland and Antarctica *Nature* **444** 195–8
Ferreira D, Marshall J, Ito T and McGee D 2018 Linking glacial-interglacial states to multiple equilibria of climate *Geophys. Res. Lett.* **45** 9160–70
Ferreira D, Marshall J and Rose B 2011 Climate determinism revisited: multiple equilibria in a complex climate model *J. Clim.* **24** 992–1012
Feudel U, Pisarchik A N and Showalter K 2018 Multistability and tipping: from mathematics and physics to climate and brain—minireview and preface to the focus issue *Chaos* **28** 033501
FitzHugh R 1961 Impulses and physiological states in theoretical models of nerve membrane *Biophys. J.* **1** 445–66
Fu R *et al* 2013 Increased dry-season length over southern Amazonia in recent decades and its implication for future climate projection *Proc. Natl Acad. Sci. USA* **110** 18110–5
Ghil M 1976 Climate stability for a sellers-type model *J. Atmos. Sci.* **33** 3–20
Ghil M 1994 Cryothermodynamics: the chaotic dynamics of paleoclimate *Physica* D **77** 130–59
Ghil M 2001 Hilbert problems for the geosciences in the 21st century *Nonlinear Process. Geophys.* **8** 211
Ghil M 2019 A century of nonlinearity in the geosciences *Earth Space Sci.* **6** 1007–42
Ghil M 2020 Review article: Hilbert problems for the climate sciences in the 21st century—20 years later *Nonlinear Process. Geophys.* **27** 429–51
Ghil M 2015 A mathematical theory of climate sensitivity or, how to deal with both anthropogenic forcing and natural variability? *Climate Change: Multidecadal and Beyond* ed C P Chang, M Ghil, M Latif and J M Wallace (Singapore: World Scientific) ch 2, pp 31–51
Ghil M, Chekroun M D and Simonnet E 2008 Climate dynamics and fluid mechanics: natural variability and related uncertainties *Physica* D **237** 2111–26
Ghil M and Childress S 1987 *Topics in Geophysical Fluid Dynamics: Atmospheric Dynamics, Dynamo Theory and Climate Dynamics* (Berlin: Springer Science+Business Media)
Ghil M, Groth A, Kondrashov D and Robertson A W 2018 Extratropical sub-seasonal-to-seasonal oscillations and multiple regimes: the dynamical systems view *The Gap Between Weather and Climate Forecasting: Sub-Seasonal to Seasonal Prediction* ed A W Robertson and F Vitart (Amsterdam: Elsevier) ch 6, pp 119–42
Ghil M and Lucarini V 2020 The physics of climate variability and climate change *Rev. Mod. Phys.* **92** 035002
Ghil M 2022 Foreword *Handbook of Climate Change Mitigation and Adaptation* 3rd edn, ed M Lackner, T Suzuki and W Chen (Springer Nature) pp VII–IX
Ghil M and Robertson A W 2002 "Waves" vs. "particles" in the atmosphere's phase space: a pathway to long-range forecasting? *Proc. Natl Acad. Sci.* **99** 2493–500
Gibbons A 1993 How the Akkadian empire was hung out to dry *Science* **261** 985
Gladwell M 2000 *The Tipping Point: How Little Things Can Make a Big Difference* (New York: Little Brown)
Good P, Boers N, Boulton C A, Lowe J A and Richter I 2021 How might a collapse in the Atlantic Meridional Overturning Circulation affect rainfall over tropical South America? *Clim. Resil. Sustain.* **1** e26
Good P, Jones C, Lowe J, Betts R and Gedney N 2013 Comparing tropical forest projections from two generations of Hadley Centre Earth System Models, HadGEM2-ES and HadCM3LC *J. Clim.* **26** 495–511
Goswami B, Boers N, Rheinwalt A, Marwan N, Heitzig J, Breitenbach S F and Kurths J 2018 Abrupt transitions in time series with uncertainties *Nat. Commun.* **9** 48
Grant E 1961 Nicole Oresme and the commensurability or incommensurability of the celestial motions *Arch. Hist. Exact Sci.* **1** 420–58
Gregory J M, George S E and Smith R S 2020 Large and irreversible future decline of the Greenland ice sheet *Cryosphere* **14** 4299–322
Gregory J M, Huybrechts P and Raper S C B 2004 Threatened loss of the Greenland ice-sheet *Nature* **428** 616
Gupta A K, Anderson D M and Overpeck J T 2003 Abrupt changes in the Asian southwest monsoon during the Holocene and their links to the North Atlantic Ocean *Nature* **421** 354–7
Hakuba M Z, Folini D, Wild M and Schr C 2012 Impact of Greenland's topographic height on precipitation and snow accumulation in idealized simulations *J. Geophys. Res.: Atmos.* **117** 1–15
Hales K, Neelin J D and Zeng N 2006 Interaction of vegetation and atmospheric dynamical mechanisms

in the mid-Holocene African monsoon *J. Clim.* **19** 4105–20
Hannachi A, Straus D M, Franzke C L E, Corti S and Woollings T 2017 Low-frequency nonlinearity and regime behavior in the Northern Hemisphere extratropical atmosphere *Rev. Geophys.* **55** 199–234
Hannart A, Pearl J, Otto F E L, Naveau P and Ghil M 2016 Causal counterfactual theory for the attribution of weather and climate-related events *Bull. Am. Meteorol. Soc.* **97** 99–110
Harris P P, Huntingford C and Cox P M 2008 Amazon Basin climate under global warming: the role of the sea surface temperature *Phil. Trans. R. Soc.* B **363** 1753–9
Hasselmann K 1976 Stochastic climate models. Part I: theory *Tellus* **28** 473–85
Hawkins E, Smith R S, Allison L C, Gregory J M, Woollings T J, Pohlmann H and de Cuevas B 2011 Bistability of the Atlantic overturning circulation in a global climate model and links to ocean freshwater transport *Geophys. Res. Lett.* **38** 1–6
Hays J D, Imbrie J and Shackleton N J 1976 Variations in the Earth's orbit: pacemaker of the ice ages *Science* **194** 1121–32
Heinrich H 1988 Origin and consequences of cyclic ice rafting in the Northeast Atlantic Ocean during the past 130,000 years *Quat. Res.* **29** 142–52
Held H and Kleinen T 2004 Detection of climate system bifurcations by degenerate fingerprinting *Geophys. Res. Lett.* **31** L23207
Held I M 2005 The gap between simulation and understanding in climate modeling *Bull. Am. Meteorol. Soc.* **86** 1609–14
Held I M and Suarez M J 1974 Simple albedo feedback models of the icecaps *Tellus* **26** 613–29
Henry L G, Mcmanus J F, Curry W B, Roberts N L, Piotrowski A M and Keigwin L D 2016 North Atlantic ocean circulation and abrupt climate change during the last glaciation *Science* **353** eaaf5529
Hirota M, Holmgren M, van Nes E H and Scheffer M 2011 Global resilience of tropical forest and savanna to critical transitions *Science* **334** 232–5
Hoffman P F *et al* 2017 Snowball Earth climate dynamics and Cryogenian geology-geobiology *Sci. Adv.* **3** e1600983
Hoffman P F, Kaufman A J, Halverson G P and Schrag D P 1998 A Neoproterozoic snowball Earth *Science* **281** 1342–6
Hoffman P F, Kaufman A J, Halverson G P and Schrag D P 2002 On the initiation of a snowball Earth *Science* **281** 1342
Hoffmann D L, Beck J W, Richards D A, Smart P L, Singarayer J S, Ketchmark T and Hawkesworth C J 2010 Towards radiocarbon calibration beyond 28 ka using speleothems from the Bahamas *Earth Planet. Sci. Lett.* **289** 1–10
Hopcroft P and Valdes P J 2021 Palaeoclimate-conditioning reveals a North Africa land-atmosphere tipping point *Proc. Natl Acad. Sci. USA* **118** 1–7
Horsthemke W and Lefever R 1984 *Noise Induced Transitions: Theory and Applications in Physics, Chemistry and Biology* (Berlin: Springer)
Hu A X, Meehl G A, Han W Q, Lu J H and Strand W G 2013 Energy balance in a warm world without the ocean conveyor belt and sea ice *Geophys. Res. Lett.* **40** 6242–6
Huntingford C *et al* 2013 Simulated resilience of tropical rainforests to CO_2-induced climate change *Nat. Geosci.* **6** 268–73
Hutchinson D K *et al* 2021 The Eocene–Oligocene transition: a review of marine and terrestrial proxy data, models and model–data comparisons *Clim. Past* **17** 269–315
Huybers P 2009 Pleistocene glacial variability as a chaotic response to obliquity forcing *Clim. Past* **5** 481–8
Imbrie J and Imbrie K P 1986 *Ice Ages: Solving the Mystery* (Cambridge, MA: Harvard University Press)
IPCC 2007 *Climate Change 2007—The Physical Science Basis: Working Group I Contribution to the Fourth Assessment Report of the IPCC* (Cambridge: Cambridge University Press)
IPCC 2013 *IPCC Fifth Assessment Report (AR5)—The Physical Science Basis* (Cambridge: Cambridge University Press)
IPCC 2021a *Climate Change 2021: The Physical Science Basis. Contribution of Working Group I to the Sixth Assessment Report of the Intergovernmental Panel on Climate Change* (Cambridge: Cambridge University Press)
IPCC 2021b Summary for Policymakers *Climate Change 2021: The Physical Science Basis. Contribution of Working Group I to the Sixth Assessment Report of the Intergovernmental Panel on Climate Change* ed V Masson-Delmotte *et al* (Cambridge: Cambridge University Press) pp 3–32
Jackson L C, Kahana R, Graham T, Ringer M A, Woollings T, Mecking J V and Wood R A 2015 Global and European climate impacts of a slowdown of the AMOC in a high resolution GCM *Clim. Dyn.* **45** 3299–316
Jackson L C and Wood R A 2018 Hysteresis and resilience of the AMOC in an eddy-permitting GCM *Geophys. Res. Lett.* **45** 8547–56
Jackson L C and Wood R A 2020 Fingerprints for early detection of changes in the AMOC *J. Clim.* **33** 7027–44
Jin F-F and Ghil M 1990 Intraseasonal oscillations in the extratropics: Hopf bifurcation and topographic instabilities *J. Atmos. Sci.* **47** 3007–22
Johnsen S J, Clausen H B, Dansgaard W, Fuhrer K, Gundestrup N, Hammer C U, Iversen P, Jouzel J, Stauffer B and Steffensen J P 1992 Irregular glacial interstadials recorded in a new Greenland ice core *Nature* **359** 311–3
Johnson G C and Lyman J M 2020 Warming trends increasingly dominate global ocean *Nat. Clim. Change* **10** 757
Jolliffe I T 2002 *Principal Component Analysis for Special Types of Data* (Berlin: Springer)
Källén E, Crafoord C and Ghil M 1979 Free oscillations in a climate model with ice-sheet dynamics *J. Atmos. Sci.* **36** 2292–303
Kanner L C, Burns S J, Cheng H and Edwards R L 2012 High-latitude forcing of the South American summer monsoon during the last glacial *Science* **335** 570–3
Kennedy A T, Farnsworth A, Lunt D J, Lear C H and Markwick P J 2015 Atmospheric and oceanic impacts of Antarctic glaciation across the Eocene–Oligocene transition *Phil. Trans. R. Soc.* A **373** 20140419
Kilic C, Lunkeit F, Raible C C and Stocker T F 2018 Stable equatorial ice belts at high obliquity in a coupled atmosphere-ocean model *Astrophys. J.* **864** 106
Kilic C, Raible C C and Stocker T F 2017 Multiple climate states of habitable exoplanets: the role of obliquity and irradiance *Astrophys. J.* **844** 147
Kindler P, Guillevic M, Baumgartner M, Schwander J, Landais A and Leuenberger M 2014 Temperature reconstruction from 10 to 120 kyr b2k from the NGRIP ice core *Clim. Past* **10** 887–902
Kjeldsen K K *et al* 2015 Spatial and temporal distribution of mass loss from the Greenland ice sheet since AD 1900 *Nature* **528** 396–400
Klockmann M, Mikolajewicz U, Kleppin H and Marotzke J 2020 Coupling of the subpolar gyre and the overturning circulation during abrupt glacial climate transitions *Geophys. Res. Lett.* **47** e2020GL090361
Knutti R and Stocker T F 2002 Limited predictability of the future thermohaline circulation close to an instability threshold *J. Clim.* **15** 179–86
Kobashi T, Severinghaus J P, Brook E J, Barnola J-M and Grachev A M 2007 Precise timing and characterization of abrupt climate change 8200 years ago from air trapped in polar ice *Quat. Sci. Rev.* **26** 1212–22
Kondrashov D, Kravtsov S, Robertson A W and Ghil M 2005 A hierarchy of data-based ENSO models *J. Clim.* **18** 4425–44
Kravtsov S, Kondrashov D and Ghil M 2009 Empirical model reduction and the modeling hierarchy in climate dynamics and the geosciences *Stochastic Physics and Climate Modeling* ed T N Palmer and P Williams (Cambridge: Cambridge University Press) pp 35–72
Kubo R 1966 The fluctuation-dissipation theorem *Rep. Prog. Phys.* **29** 255–84

Kuehn C, Lux K and Neamtu A 2022 Warning signs for non-Markovian bifurcations: colour blindness and scaling laws *Proc. R. Soc.* A **478** 20210740
Lackner M, Sajjadi B and Chen W-Y (eds) 2022 *Handbook of Climate Change Mitigation and Adaptation* 3rd edn (New York: Springer Nature)
Ladant J-B, Donnadieu Y, Lefebvre V and Dumas C 2014 The respective role of atmospheric carbon dioxide and orbital parameters on ice sheet evolution at the Eocene–Oligocene transition *Paleoceanography* **29** 810–23
Laskar J, Robutel P, Joutel F, Gastineau M, Correia A C M and Levrard B 2004 A long-term numerical solution for the insolation quantities of the Earth *Astron. Astrophys.* **428** 261–85
Lenton T M, Held H, Kriegler E, Hall J W, Lucht W, Rahmstorf S and Schellnhuber H J 2008 Tipping elements in the Earth's climate system *Proc. Natl Acad. Sci.* **105** 1786–93
Levermann A, Schewe J, Petoukhov V and Held H 2009 Basic mechanism for abrupt monsoon transitions *Proc. Natl Acad. Sci. USA* **106** 20572–7
Levermann A and Winkelmann R 2016 A simple equation for the melt elevation feedback of ice sheets *Cryosphere* **10** 1799–807
Lisiecki L E and Raymo M E 2005 A Pliocene-Pleistocene stack of 57 globally distributed benthic δ^{18}O records *Paleoceanography* **20** 1–17
Liu W, Liu Z and Brady E C 2014 Why is the AMOC monostable in coupled general circulation models? *J. Clim.* **27** 2427–43
Liu W, Xie S-P, Liu Z and Zhu J 2017 Overlooked possibility of a collapsed Atlantic Meridional Overturning Circulation in warming climate *Sci. Adv.* **3** e1601666
Lorenz E N 1963a Deterministic nonperiodic flow *J. Atmos. Sci.* **20** 130–41
Lorenz E N 1963b The mechanics of vacillation *J. Atmos. Sci.* **20** 448–64
Manabe S and Stouffer R J 1988 Two stable equilibria of a coupled ocean–atmosphere model *J. Clim.* **1** 841–66
Mann M E, Steinman B A and Miller S K 2020 Absence of internal multidecadal and interdecadal oscillations in climate model simulations *Nat. Commun.* **11** 49
Marengo J A, Souza C M, Thonicke K, Burton C, Halladay K, Betts R A, Alves L M and Soares W R 2018 Changes in climate and land use over the Amazon region: current and future variability and trends *Front. Earth Sci.* **6** 1–21
Marengo J A, Tomasella J, Alves L M, Soares W R and Rodriguez D A 2011 The drought of 2010 in the context of historical droughts in the Amazon region *Geophys. Res. Lett.* **38** 1–5
Mecking J V, Drijfhout S S, Jackson L C and Andrews M B 2017a The effect of model bias on Atlantic freshwater transport and implications for AMOC bi-stability *Tellus* A **69** 1–15
Mecking J V, Drijfhout S S, Jackson L C and Andrews M B 2017b The effect of model bias on Atlantic freshwater transport and implications for AMOC bi-stability *Tellus* A **69** 1–15
Mecking J V, Drijfhout S S, Jackson L C and Graham T 2016 Stable AMOC off state in an eddy-permitting coupled climate model *Clim. Dyn.* **47** 2455–70
Milankovitch M 1920 *Théorie Mathématique des Phénomènes Thermiques Produits par la Radiation Solaire* (Paris: Gauthier-Villars)
Mosblech N A, Bush M B, Gosling W D, Hodell D, Thomas L, van Calsteren P, Correa-Metrio A, Valencia B G, Curtis J and van Woesik R 2012 North Atlantic forcing of Amazonian precipitation during the last ice age *Nat. Geosci.* **5** 817–20
Mouginot J, Rignot E, Bjork A A, van den Broeke M, Millan R, Morlighem M, Noel B, Scheuchl B and Wood M 2019 Forty-six years of Greenland Ice Sheet mass balance from 1972 to 2018 *Proc. Natl Acad. Sci. USA* **116** 9239–44
Nagumo J, Arimoto S and Yoshizawa S 1962 An active pulse transmission line simulating nerve axon *Proc. IRE* **50** 2061–70
NGRIP Members 2004 High-resolution record of Northern Hemisphere climate extending into the last interglacial period *Nature* **431** 147–51
Nicolis C 1981 Solar variability and stochastic effects on climate *Sol. Phys.* **74** 473–8
North G R, Howard L, Pollard D and Wielicki B 1979 Variational formulation of Budyko–Sellers climate models *J. Atmos. Sci.* **36** 255–9
Oeschger H, Beer J, Siegenthaler U, Stauffer B, Dansgaard W and Langway C 1984 Late glacial climate history from ice cores *Climate Processes and Climate Sensitivity* (*Geophysical Monograph Series* vol 29) ed J E Hansen and T Takahashi (Washington, DC: American Geophysical Union) pp 299–306
Ogutu K, D'Andrea F, Groth A and Ghil M 2022 Coupled climate-economy-ecology modeling: a dynamic and stochastic approach *Handbook of Climate Change Mitigation and Adaptation* 3rd edn, ed M Lackner, T Suzuki and W-Y Chen (New York: Springer Nature) ch 6, pp 225–87
Palmer T and Stevens B 2019 The scientific challenge of understanding and estimating climate change *Proc. Natl Acad. Sci. USA* **116** 34390–5
Parsons L A 2020 Implications of CMIP6 projected drying trends for 21st century Amazonian drought risk *Earth's Future* **8** e2020EF001608
Parsons L A, Yin J, Overpeck J T, Stouffer R J and Malyshev S 2014 Influence of the Atlantic Meridional Overturning Circulation on the monsoon rainfall and carbon balance of the American tropics *Geophys. Res. Lett.* **41** 146–51
Pedro J, Jochum M, Buizert C, He F, Barker S and Rasmussen S 2018 Beyond the bipolar seesaw: toward a process understanding of interhemispheric coupling *Quat. Sci. Rev.* **192** 27–46
Peltier W R and Vettoretti G 2014 Dansgaard–Oeschger oscillations predicted in a comprehensive model of glacial climate: a "kicked" salt oscillator in the Atlantic *Geophys. Res. Lett.* **41** 7306–13
Pierini S and Ghil M 2021 Tipping points induced by parameter drift in an excitable ocean model *Sci. Rep.* **11** 11126
Pierrehumbert R T 2005 Climate dynamics of a hard snowball Earth *Geophys. Res. Lett.* **110** D01111
Quon C and Ghil M 1992 Multiple equilibria in thermosolutal convection due to salt-flux boundary conditions *J. Fluid Mech.* **245** 449–83
Rahmstorf S 2002 Ocean circulation and climate during the past 120,000 years *Nature* **419** 207–14
Rahmstorf S *et al* 2005 Thermohaline circulation hysteresis: a model intercomparison *Geophys. Res. Lett.* **32** L23605
Rasmussen S O *et al* 2014 A stratigraphic framework for abrupt climatic changes during the Last Glacial period based on three synchronized Greenland ice-core records: refining and extending the INTIMATE event stratigraphy *Quat. Sci. Rev.* **106** 14–28
Richardson P L 2008 On the history of meridional overturning circulation schematic diagrams *Prog. Oceanogr.* **76** 466–86
Riechers K, Mitsui T, Boers N and Ghil M 2021 Orbital insolation variations, intrinsic climate variability and quaternary glaciations *Clim. Past* **18** 863–93
Rignot E, Mouginot J, Scheuchl B, van den Broeke M, van Wessem M J and Morlighem M 2019 Four decades of Antarctic Ice Sheet mass balance from 1979–2017 *Proc. Natl Acad. Sci. USA* **116** 1095–103
Robertson A W, Farrara J D and Mechoso C R 2003 Simulations of the atmospheric response to South Atlantic sea surface temperature anomalies *J. Clim.* **16** 2540–51
Robinson A, Calov R and Ganopolski A 2012 Multistability and critical thresholds of the Greenland ice sheet *Nat. Clim. Change* **2** 429–32
Rodwell M J and Hoskins B J 2001 Subtropical anticyclones and summer monsoons *J. Clim.* **14** 3192–211
Rombouts J and Ghil M 2015 Oscillations in a simple climate–vegetation model *Nonlinear Process. Geophys.* **22** 275–88
Roques L, Chekroun M, Cristofol M, Soubeyrand S and Ghil M 2014 Parameter estimation for energy balance models with memory *Proc. R. Soc.* A **470** 20140349

Rousseau D D, Boers N, Sima A, Svensson A, Bigler M, Lagroix F, Taylor S and Antoine P 2017 (MIS3 & 2) millennial oscillations in Greenland dust and Eurasian Aeolian records—a paleosol perspective *Quat. Sci. Rev.* **169** 99–113
Rousseau D-D, Bagniewski W and Ghil M 2022 Abrupt climate changes and the astronomical theory: are they related? *Clim. Past* **18** 249–71
Ryan J C, Smith L C, van As D, Cooley S W, Cooper M G, Pitcher L H and Hubbard A 2019 Greenland ice sheet surface melt amplified by snowline migration and bare ice exposure *Sci. Adv.* **5** eaav3738
Rypdal M 2016 Early-warning signals for the onsets of Greenland interstadials and the Younger Dryas–Preboreal transition *J. Clim.* **29** 4047–56
Saltzman B and Maasch K A 1991 A first-order global model of late Cenozoic climatic change. II. Further analysis based on a simplification of CO_2 dynamics *Clim. Dyn.* **5** 201–10
Scheffer M, Bascompte J, Brock W A, Brovkin V, Carpenter S R, Dakos V, Held H, van Nes E H, Rietkerk M and Sugihara G 2009 Early-warning signals for critical transitions *Nature* **461** 53–59
Schneider S H and Dickinson R E 1974 Climate modelling *Rev. Geophys. Space Phys.* **25** 447–93
Schoof C 2007 Ice sheet grounding line dynamics: steady states, stability and hysteresis *J. Geophys. Res.: Earth Surf.* **112** F3
Sellers W D 1969 A global climatic model based on the energy balance of the Earth atmosphere *J. Appl. Meteorol.* **8** 392–400
Shepherd A *et al* 2018 Mass balance of the Antarctic ice sheet from 1992 to 2017 *Nature* **558** 219–22
Simonnet E, Dijkstra H A and Ghil M 2009 Bifurcation analysis of ocean, atmosphere and climate models *Computational Methods for the Ocean and the Atmosphere* ed R Temam and J J Tribbia (Amsterdam: Elsevier) pp 187–229
Smith T, Traxl D and Boers N 2022 Satellite-based evidence for global loss of vegetation resilience *Nat. Clim. Change* **14** 477–84
Spracklen D V and Garcia-Carreras L 2015 The impact of Amazonian deforestation on Amazon basin rainfall *Geophys. Res. Lett.* **42** 9546–52
Stanley J-D, Krom M D, Cliff R A and Woodward J C 2003 Short contribution: Nile flow failure at the end of the Old Kingdom, Egypt: strontium isotopic and petrologic evidence *Geoarchaeology* **18** 395–402
Steffensen J P *et al* 2008 High-resolution Greenland ice core data show abrupt climate change happens in few years *Science* **321** 680–4
Stocker T F 2000 Past and future reorganisations in the climate system *Quat. Sci. Rev.* **19** 301–19
Stocker T F and Johnsen S 2003 A minimum thermodynamic model for the pibolar seesaw *Paleoceanography* **18** 1087
Stocker T F and Schmittner A 1997 Influence of CO_2 emission rates on the stability of the thermohaline circulation *Nature* **388** 862–5
Stocker T F and Wright D G 1991 Rapid transitions of the ocean's deep circulation induced by changes in surface water fluxes *Nature* **351** 729–32
Stocker T F, Wright D G and Mysak L A 1992 A zonally averaged, coupled ocean-atmosphere model for paleoclimate studies *J. Clim.* **5** 773–97
Stommel H 1961 Thermohaline convection with two stable regimes of flow *Tellus* **2** 244–230
Stouffer R J *et al* 2006 Investigating the causes of the response of the thermohaline circulation to past and future climate changes *J. Clim.* **19** 1365–87
Strogatz S H 2018 *Nonlinear Dynamics and Chaos: With Applications to Physics, Biology, Chemistry and Engineering* (Boca Raton, FL: CRC Press)
Strong C, Jin F-F and Ghil M 1995 Intraseasonal oscillations in a barotropic model with annual cycle and their predictability *J. Atmos. Sci.* **52** 2627–42
Summerhayes C P 2015 *Earth's Climate Evolution: A Geological Perspective* (New York: Wiley)
Sura P 2002 Noise-induced transitions in a barotropic β-plane channel *J. Atmos. Sci.* **59** 97–110
Svensson A *et al* 2020 Bipolar volcanic synchronization of abrupt climate change in Greenland and Antarctic ice cores during the last glacial period *Clim. Past* **16** 1565–80
Thornalley D J R *et al* 2018 Anomalously weak Labrador Sea convection and Atlantic overturning during the past 150 years *Nature* **556** 227–30
Valdes P 2011 Built for stability *Nat. Geosci.* **4** 414–6
van der Pol B 1920 A theory of the amplitude of free and forced triode vibrations *Radio Rev.* **1** 701–10
van der Pol B 1926 On relaxation-oscillations *London, Edinburgh Dublin Phil. Mag. J. Sci.* **2** 978–92
Varadi F, Runnegar B and Ghil M 2003 Successive refinements in long-term integrations of planetary orbits *Astrophys. J.* **592** 620–30
Veronis G 1963 An analysis of the wind-driven ocean circulation with a limited number of Fourier components *J. Atmos. Sci.* **20** 577–93
Vettoretti G and Peltier W R 2016 Thermohaline instability and the formation of glacial North Atlantic super polynyas at the onset of Dansgaard–Oeschger warming events *Geophys. Res. Lett.* **43** 5336–44
von der Heydt A S, Dijkstra H A, van de Wal R S W, Caballero R, Crucifix M, Foster G L, Huber M, Köhler P, Rohling E and Valdes P J E 2016 Lessons on climate sensitivity from past climate changes *Curr. Clim. Change Rep.* **2** 148–58
Wang Y, Cheng H, Edwards R L, Kong X, Shao X, Chen S, Wu J, Jiang X, Wang X and An Z 2008 Millennial- and orbital-scale changes in the East Asian monsoon over the past 224,000 years *Nature* **451** 18–21
Weeks E R, Tian Y, Urbach J S, Ide K, Swinney H L and Ghil M 1997 Transitions between blocked and zonal flows in a rotating annulus with topography *Science* **278** 1598–601
Weertman J 1961 Stability of ice-age ice sheets *J. Geophys. Res.* **66** 3783–92
Weijer W, Cheng W, Drijfhout S S, Fedorov A V, Hu A, Jackson L C, Liu W, McDonagh E L, Mecking J V and Zhang J 2019 Stability of the Atlantic Meridional Overturning Circulation: a review and synthesis *J. Geophys. Res.: Oceans* **124** 5336–75
Westerhold T *et al* 2020 An astronomically dated record of Earth's climate and its predictability over the last 66 million years *Science* **369** 1383–7
Wetherald R T and Manabe S 1975 The effects of changing the solar constant on the climate of a general circulation model *J. Atmos. Sci.* **32** 2044–59
Wieczorek S, Ashwin P, Luke C M and Cox P M 2011 Excitability in ramped systems: the compost-bomb instability *Proc. R. Soc.* A **467** 1243–69
Zaliapin I and Ghil M 2010 Another look at climate sensitivity *Nonlinear Process. Geophys.* **17** 113–22
Zhang X, Lohmann G, Knorr G and Purcell C 2014 Abrupt glacial climate shifts controlled by ice sheet changes *Nature* **512** 290–4